

1 **DNA methylation across the genome in aged human skeletal muscle tissue and stem cells: The**
2 **role of HOX genes and physical activity**

3
4 Turner DC^{#1,2,3}, Gorski PP^{#1,3}, Maasar MF⁴, Seaborne RA^{2,3,6}, Baumert P^{4,5}, Brown AD², Kitchen MO³, Erskine
5 RM^{4,7}, Dos-Remedios I⁸, Voisin S⁹, Eynon N⁹, Sultanov RI¹⁰, Borisov OV^{10,11}, Larin AK¹⁰, Semenova EA¹⁰,
6 Popov DV¹², Generozov EV¹⁰, Stewart CE², Drust B¹⁴, Owens DJ^{2,4}, Ahmetov IJ^{§4,13,15}, Sharples AP^{*1,2,3}

7 ¹ Department for Physical Performance, Norwegian School of Sport Sciences (NiH), Oslo, Norway.

8 ² Stem Cells, Ageing and Molecular Physiology Unit, Exercise Metabolism and Adaptation Research Group, Research
9 Institute for Sport and Exercise Sciences, Liverpool John Moores University, Liverpool, United Kingdom.

10 ³ Institute for Science and Technology in Medicine (ISTM), School of Pharmacy & Bioengineering, Keele University,
11 Staffordshire, United Kingdom.

12 ⁴ Exercise Metabolism and Adaptation Research Group, Research Institute for Sport and Exercise Sciences, Liverpool
13 John Moores University, Liverpool, United Kingdom.

14 ⁵ Exercise Biology Group, Faculty of Sport and Health Sciences, Technical University of Munich, Munich, Germany.

15 ⁶ Centre for Genomics and Child Health, Blizard Institute, Barts and the London School of Medicine and Dentistry, Queen
16 Mary University of London, London, United Kingdom.

17 ⁷ Institute of Sport, Exercise and Health, University College London, London, United Kingdom

18 ⁸ Orthopedics Department, University Hospitals of the North Midlands, Staffordshire, UK.

19 ⁹ Institute for Health and Sport (iHeS), Victoria University, Footscray, Victoria, Australia.

20 ¹⁰ Department of Molecular Biology and Genetics, Federal Research and Clinical Center of Physical-Chemical Medicine
21 of Federal Medical Biological Agency, Moscow, Russia.

22 ¹¹ Institute for Genomic Statistics and Bioinformatics, University Hospital Bonn, Bonn, Germany

23 ¹² Laboratory of Exercise Physiology, Institute of Biomedical Problems of the Russian Academy of Sciences, Moscow,
24 Russia.

25 ¹³ Laboratory of Molecular Genetics, Kazan State Medical University, Kazan, Russia.

26 ¹⁴ School of Sport, Exercise and Rehabilitation Sciences, College of Life and Environmental Sciences, University of
27 Birmingham.

28 ¹⁵ Department of Physical Education, Plekhanov Russian University of Economics, Moscow, Russia

29

30

31 #These authors contributed equally to the work.

32

33 *Corresponding author for Skeletal muscle tissue, stem cells and DNA / HOX methylation

34 a.p.sharples@googlemail.com

35 § Corresponding author for physical activity and HOX methylation

36 I.Ahmetov@ljmu.ac.uk

37

38 **Abstract**

39

40 Skeletal muscle tissue demonstrates global hypermethylation with aging. However, methylome changes
41 across the time-course of differentiation in aged human muscle derived stem cells, and larger coverage arrays
42 in aged muscle tissue have not been undertaken. Using 850K DNA methylation arrays we compared the
43 methylomes of young (27 ± 4.4 years) and aged (83 ± 4 years) human skeletal muscle and that of young/aged
44 muscle stem cells over several time points of differentiation (0, 72 hours, 7, 10 days). Aged muscle tissue was
45 hypermethylated compared with young tissue, enriched for; 'pathways-in-cancer' (including; focal adhesion,
46 MAPK signaling, PI3K-Akt-mTOR signaling, p53 signaling, Jak-STAT signaling, TGF-beta and notch signaling),
47 'rap1-signaling', 'axon-guidance' and 'hippo-signalling'. Aged muscle stem cells also demonstrated a
48 hypermethylated profile in pathways; 'axon-guidance', 'adherens-junction' and 'calcium-signaling',
49 particularly at later timepoints of myotube formation, corresponding with reduced morphological
50 differentiation and reductions in MyoD/Myogenin gene expression compared with young cells. While young
51 cells showed little alteration in DNA methylation during differentiation, aged cells demonstrated extensive
52 and significantly altered DNA methylation, particularly at 7 days of differentiation and most notably in the
53 'focal adhesion' and 'PI3K-AKT signalling' pathways. While the methylomes were vastly different between
54 muscle tissue and isolated muscle stem cells, we identified a small number of CpG sites showing a
55 hypermethylated state with age, in both muscle and tissue and stem cells (on genes *KIF15*, *DYRK2*, *FHL2*,
56 *MRPS33*, *ABCA17P*). Most notably, differential methylation analysis of chromosomal regions identified three
57 locations containing enrichment of 6-8 CpGs in the HOX family of genes altered with age. With *HOXD10*,
58 *HOXD9*, *HOXD8*, *HOXA3*, *HOXC9*, *HOXB1*, *HOXB3*, *HOXC-AS2* and *HOXC10* all hypermethylated in aged tissue.
59 In aged cells the same HOX genes (and additionally *HOXC-AS3*) displayed the most variable methylation at 7
60 days of differentiation versus young cells, with *HOXD8*, *HOXC9*, *HOXB1* and *HOXC-AS3* hypermethylated and
61 *HOXC10* and *HOXC-AS2* hypomethylated. We also determined that there was an inverse relationship
62 between DNA methylation and gene expression for *HOXB1*, *HOXA3* and *HOXC-AS3*. Finally, increased physical
63 activity in young adults was associated with oppositely regulating *HOXB1* and *HOXA3* methylation compared
64 with age. Overall, we demonstrate that a considerable number of HOX genes are differentially epigenetically
65 regulated in aged human skeletal muscle and muscle stem cells and increased physical activity may help
66 prevent age-related epigenetic changes in these HOX genes.

67

68

69

70

71

72 **Keywords:** Epigenetics, Aging, DNA methylation, Exercise

73

74 Introduction

75

76 Maintaining skeletal muscle mass and function into older age is fundamental for human health-span and
77 quality of life ¹. Five to ten percent of older humans have sarcopenia ^{2,3}, which is characterized by reductions
78 in muscle mass and strength ⁴. This loss of muscle mass and strength leads to frailty, increased incidence of
79 falls, hospitalization and morbidity ^{4,5,6,7,8,9,10,11}. Annual costs of fragility are estimated to be 39/32 billion
80 (Euros/USD) for European and USA fragility fractures respectively, with the cost of sarcopenia estimated to
81 be £2 billion in the UK ¹². With an ageing population, these costs are likely to increase with time.

82

83 A primary hallmark of ageing is the alteration of the epigenetic landscape. Epigenetics encompasses the
84 interaction between lifestyle/environmental factors and modifications to DNA and histones, without changes
85 to the inherited DNA sequence ^{13,14}. DNA methylation is the most studied epigenetic modification and
86 involves the addition of a covalent methyl group to the 5' position of the pyrimidine ring of a cytosine (5mC).
87 Increased methylation (hypermethylation) to cytosine-guanine (C-G) pairings (CpG sites), especially in CpG-
88 rich regions such as gene promoters, typically leads to reduced capacity for the transcriptional apparatus to
89 bind to these regions, suppressing gene expression ¹⁴. Methylated CpG islands in promoters also leads to a
90 tight compaction of adjacent chromatin via the recruitment of chromatin modifying protein/protein-
91 complexes, further silencing gene expression. In contrast, reduced methylation (hypomethylation) provides
92 a more favorable DNA landscape for the transcriptional apparatus to bind to these regions, as well as more
93 'relaxed' chromatin, enabling gene expression to occur.

94

95 DNA methylation in aged skeletal muscle occurs at tissue-specific genes ¹⁵. However, aged muscle also has
96 the smallest overlap with other aged tissue types, suggesting skeletal muscle is unique in comparison with
97 other tissues in its epigenetic aging processes ¹⁵. Indeed, it has recently been demonstrated that the
98 methylation status of approximately 200 CpG sites can accurately predict chronological age in skeletal muscle
99 tissue ¹⁶. But that this muscle 'clock' only shares 16 of these CpG's with the original 353 CpG pan-tissue
100 Horvath clock ^{16,17}. Further, using DNA methylation arrays with coverage of ~450,000 CpG sites ¹⁸, Zykovich
101 *et al.* demonstrated that compared with young human skeletal muscle, aged skeletal muscle is
102 hypermethylated across the genome. Moreover, our group has demonstrated that mouse skeletal muscle
103 stem cells exposed to a high dose of inflammatory stress in early proliferative life retained hypermethylation
104 of *MyoD* (a muscle-specific regulatory factor) 30 population doublings later ¹⁹. This suggests that inflamed
105 proliferative aging in muscle stem cells leads to a retained accumulation of DNA methylation. Finally, lifelong
106 physical activity ²⁰, endurance and resistance exercise ²⁰ have been associated with predominantly
107 hypomethylation of the genome in young skeletal muscle ^{21,22}. This contrasts with the hypermethylation
108 observed with aging, suggesting that exercise may reverse some age-related changes in DNA methylation.

109

110 Skeletal muscle fibers are post-mitotic as they contain terminally differentiated/fused nuclei (myonuclei);
111 thus, repair and regeneration of skeletal muscle tissue is mediated by a separate population of resident stem
112 cells (satellite cells) that can divide. Once activated, satellite cells proliferate and migrate to the site of injury
113 to differentiate and fuse with the existing fibers to enable repair. Target gene analysis showed altered DNA
114 methylation during differentiation of muscle cells into myotubes *in-vitro*²³. This included altered methylation
115 of MyoD²⁴, Myogenin²⁵ and Six1²⁶. While muscle stem cells derived from aged individuals display similar
116 proliferative capacity and time to senescence as young adult cells^{27,28}, they do have impaired differentiation
117 and fusion into myotubes^{29, 30, 31, 32, 33, 34, 35, 36, 37, 38, 39, 40, 41, 42, 43, 44, 45}. However, a small number of studies did
118 not find an effect of age on the differentiation capacity of isolated cells^{27, 46, 47}. A single study assessed DNA
119 methylation across the genome (450K CpG sites) in aged versus young adult muscle stem cells²⁷ and showed
120 genome-wide hypermethylation in aged cells as well as aged tissue²⁷.

121

122 To date, there has been no report of genome-wide DNA methylation dynamics during the entire time-course
123 of muscle cell differentiation, or how age modulates these dynamics. Furthermore, the latest, larger coverage
124 methylation arrays have not yet been implemented in aged muscle tissue. Therefore, the objectives of the
125 current study were: 1) To describe the dynamics of the human DNA methylome in aged and young adult
126 skeletal muscle tissue and primary muscle-derived stem cells over an extensive time-course of
127 differentiation; 0 h (30 minutes post transfer to differentiation media), 72 h (hours), 7 d (days) and 10 d using
128 high coverage 850K CpG arrays. 2) To identify if methylation patterns are similar or different in muscle stem
129 cells compared to skeletal muscle tissue. 3) To test whether increasing physical activity levels is associated
130 with altering DNA methylation in the same genes in aged muscle.

131

132 **Methods**

133

134 *Skeletal muscle biopsies and primary cell isolations*

135 For young adults (n = 9, male, 27 ± 4.4 years-old), skeletal muscle tissue (~150 mg) was obtained from the
136 vastus lateralis via a conchotome biopsy. Consent and ethical approval were granted for the collection of
137 muscle tissue under NREC, UK approval (16/WM/010) or LJMU, UK local ethics committee approvals
138 [H19/SPS/028 & H15/SPS/031]. Six (out of 9) of the young adult's tissue (male, 28 ± 5.3 years) baseline (at
139 rest) array data was derived from Seaborne *et al.* (2018). This is because we used this baseline tissue to derive
140 cells (detailed below) for DNA methylation analysis of stem cell experiments in the present study. For older
141 adults (n = 5, 2 men/3 women, 83 ± 4 years), tissue biopsies were obtained during elective orthopedic
142 surgeries from University Hospitals of the North Midlands, from the vastus lateralis (knee surgery, n = 2) or
143 gluteus medius muscles (hip surgery, n = 3), under consent and ethical approval 18/WM/0187. DNA and RNA
144 were isolated from these young and aged tissue samples. DNA samples from all 9 young and 5 aged adults
145 were analysed for DNA methylation arrays (detailed below), and a subset were analysed for gene expression

146 (young n = 4, aged n = 5). Primary skeletal muscle cells were derived from a subset of young adult and aged
147 tissue samples, and isolated as per our previous work ^{21, 22, 48, 49, 50, 51}. Briefly, approximately 100 mg biopsy
148 tissue was immediately (~10-30 mins) transferred to a sterile class II biological safety cabinet in pre-cooled
149 (4°C) transfer media (Hams F-10, 2% hi-FBS, 100 U/ml penicillin, 100 µg/ml streptomycin and 2.5 µg/ml
150 amphotericin-B). Any visible connective and adipose tissue were removed using sterile scalpels and muscle
151 tissue was thoroughly washed 2 × in sterile PBS (containing 100 U/ml penicillin, 100 µg/ml streptomycin, 2.5
152 µg/ml amphotericin-B). PBS was removed and the muscle tissue was minced in the presence of 0.05%
153 Trypsin/0.02% EDTA and all contents (tissue and trypsin) were transferred to a magnetic stirring platform at
154 37°C for 10 minutes. The addition of 0.05% Trypsin/0.02% EDTA and titration was repeated on any remaining
155 tissue. The supernatant was collected from both procedures and horse serum (HS) was added at 10% of the
156 total supernatant volume to neutralize the trypsin. The supernatant was centrifuged at 340 g for 5 minutes
157 where the supernatant and cell pellet were both plated in separate pre-gelatinised (0.2% gelatin) T25 flasks
158 containing 7.5 ml fresh pre-heated growth media/GM (GM; Ham's F10 nutrient mix supplemented with 10%
159 hi-NCS, 10% hi-FBS, 100 U/ml penicillin, 100 µg/ml streptomycin, 2.5 µg/ml amphotericin B and 5 mM L-
160 glutamine). Once confluent, cells were trypsinised and reseeded into larger T75's to expand the cell
161 population. Human derived muscle cells (HMDCs) were seeded onto gelatin coated 6 well plates, at a density
162 of 9×10^5 cells/ml in 2 ml of GM for until ~90% confluency was attained (~48 h). GM was removed, and cells
163 underwent 3 × PBS washes before switching to low serum differentiation media (DM; Ham's F10 nutrient mix
164 supplemented with 2% hiFBS, 100 U/ml penicillin, 100 µg/ml streptomycin, 2.5 µg/ml amphotericin B and 5
165 mM L-glutamine). HMDCs were differentiated for a total of 10 days (d) which received a 1 ml top up of DM
166 at 72 h and 7 d timepoints. Cells were lysed for DNA and RNA at 0 h (30 minutes in DM), 72 h, 7 d and 10 d,
167 at the same time of day (approx. 08.00-11.00) to minimize the impact of circadian oscillation ⁵². All
168 experiments were carried out below passage 10 to prevent senescence. We undertook methylation arrays
169 on DNA isolated from: 0 h young (n = 7), 0 h aged (n = 4), 72 h young (n = 7), 72 h aged (n = 4), 7 d young (n
170 = 6), 7d aged (n = 3), 10 d young (n = 2) and 10 d aged (n= 4). Gene expression was analysed using young (n
171 = 4, 7 d) and aged (n = 3, 7 d) cells. It's worth noting that we had n= 3-4 for most conditions, however in the
172 10 d young cells condition, the DNA did not pass QA/QC for the arrays, and we had no cells left for these
173 participants. Therefore, unfortunately we could only run n = 2 for this single condition. Therefore, results for
174 this condition should be viewed with this caveat in mind. A schematic of experimental design can be found
175 in Suppl. Figure 1.

176

177 *Myogenicity and morphology measurements*

178 Following isolations, attached single cells were fixed prior to staining and fluorescent immunocytochemistry
179 analysis to determine myogenicity (via desmin positivity) of the isolated young and aged muscle derived
180 cultures. Briefly, approximately 2×10^4 cells were seeded onto 3 × wells of a 6-well plate and were incubated
181 for 24 h in GM. Existing media was removed and cells were washed 3 × in PBS before fixation using the graded

182 methanol/acetone method (50:25:25 TBS:methanol:acetone for 15 minutes followed by 50:50
183 methanol:acetone) after which cells were permeabilised in 0.2% Triton X-100 and blocked in 5% goat serum
184 (Sigma-Aldrich, UK) in TBS for 30 minutes. Cells were washed 3 × in TBS and incubated overnight (4 °C) in 300
185 µl of TBS (with 2% goat serum and 0.2% Triton X-100) containing primary anti-desmin antibody (1:50;
186 ab15200, Abcam, UK). After overnight incubation, cells were washed 3 × in TBS and incubated at RT for 3 h
187 in 300 µl of secondary antibody solution (TBS, 2% goat serum and 0.2% Triton X-100) containing the
188 secondary antibody, anti-rabbit TRITC (1:75; T6778, Sigma-Aldrich, UK) to counterstain desmin. Finally, cells
189 were washed again 3 × in TBS, prior to counterstaining nuclei using 300 µl of DAPI solution at a concentration
190 of (300 nM; D1306, Thermo Fisher Scientific, UK) for 30 minutes. Immunostained cells were then visualised
191 using a fluorescent microscope (Nikon, Eclipse Ti-S, Japan or Olympus IX83, Japan) and imaged using
192 corresponding software (Nikon, NIS Elements and Olympus FV10-ASW 4.2). Myoblasts, myotubes and nuclei
193 were visualized using TRITC (Desmin, Excitation: 557 nm, Emission: 576 nm) DAPI (Excitation: 358 nm,
194 Emission: 461 nm) filter cubes. All immunostained samples were imported to Fiji/ImageJ (version 2.0.0)
195 software for subsequent calculations. Note, there was no difference ($p = 0.86$) in myogenic cell proportions
196 in aged ($35 \pm 5\%$) versus young cells ($34 \pm 9\%$). Therefore, the aged and young muscle derived cells were
197 matched for their desmin positivity (% myoblasts) prior to differentiation experiments and downstream DNA
198 methylation and gene expression analysis. To determine myotube differentiation and formation at each time
199 point, cells were imaged using light microscopy (Olympus, CKX31, Japan) at 0, 72 h, 7 and 10 d of
200 differentiation.

201

202 *DNA isolation and bisulfite conversion*

203 Prior to DNA isolation, tissue samples were homogenized for 45 seconds at 6,000 rpm × 3 (5 minutes on ice
204 in between intervals) in lysis buffer (180 µl buffer ATL with 20 µl proteinase K) provided in the DNeasy spin
205 column kit (Qiagen, UK) using a Roche Magnalyser instrument and homogenization tubes containing ceramic
206 beads (Roche, UK). DNA was then isolated using the DNAeasy kit (Qiagen, UK) according to manufacturer's
207 instructions. Cells were lysed in 180 µl PBS containing 20 µl proteinase K, scraped from wells, and then
208 isolated using DNAeasy kits (Qiagen, UK) as above with the tissue lysates. The DNA was then bisulfite
209 converted using the EZ DNA Methylation Kit (Zymo Research, CA, United States) as per manufacturer's
210 instructions.

211

212 *Infinium MethylationEPIC BeadChip Array*

213 All DNA methylation experiments were performed in accordance with Illumina manufacturer instructions for
214 the Infinium MethylationEPIC 850K BeadChip Array (Illumina, USA). Methods for the amplification,
215 fragmentation, precipitation and resuspension of amplified DNA, hybridisation to EPIC beadchip, extension
216 and staining of the bisulfite converted DNA (BCD) can be found in detail in our open access methods paper
217 ⁴⁹. EPIC BeadChips were imaged using the Illumina iScan® System (Illumina, United States).

218

219 *DNA methylation analysis, CpG enrichment analysis (GO and KEGG pathways), differentially modified region*
220 *analysis and Self Organising Map (SOM) profiling*

221 Following DNA methylation quantification via MethylationEPIC BeadChip array, raw .IDAT files were
222 processed using Partek Genomics Suite V.7 (Partek Inc. Missouri, USA) and annotated using the
223 MethylationEPIC_v-1-0_B4 manifest file. We first checked the average detection p-values. The highest
224 average detection p-value for the samples was 0.0023 (Suppl. Figure **2a**), which is well below the
225 recommended 0.01 in the Oshlack workflow⁵³. We also produced density plots of the raw intensities/signals
226 of the probes (Suppl. Figure **2b**). These demonstrated that all methylated and unmethylated signals were
227 over 11.5 (mean was 11.52 and median was 11.8), and the difference between median methylation and
228 median unmethylated signal was 0.56⁵³. Upon import of the data into Partek Genomics Suite we removed
229 probes that spanned X and Y chromosomes from the analysis due to having both males and females in the
230 study design, and although the average detection p-value for each samples was on average very low (no
231 higher than 0.0023) we also excluded any individual probes with a detection p-value that was above 0.01 as
232 recommended in⁵³. Out of a total of 865,860 probes, removal of the X and Y chromosome probes and those
233 with a detection p-value above 0.01 reduced the probe number to 846,233 (removed 19,627 probes). We
234 also filtered out probes located in known single-nucleotide polymorphisms (SNPs) and any known cross-
235 reactive probes using previously defined SNP and cross-reactive probe lists identified in earlier 850K
236 validation studies⁵⁴. This resulted in a final list of 793,200 probes to be analysed. Following this, background
237 normalisation was performed via functional normalisation (with noob background correction), as previously
238 described⁵⁵. Following functional normalisation, we also undertook quality control procedures of principle
239 component analysis (PCA), density plots by lines as well as box and whisker plots of the normalised data for
240 tissue samples (Suppl. Figures **2c, d, e** respectively) and cell samples (Suppl. Figures **2 f, g, h** respectively).
241 Any outlier samples were detected using PCA and the normal distribution of β -values. Outliers were then
242 removed if they fell outside 2 standard deviations (SDs) (e.g. Suppl. Figure **2c**) of the ellipsoids and/or if they
243 demonstrated different distribution patterns to the samples of the same condition. Only one young adult
244 male tissue sample was removed due to being outside 2 standard deviations outside samples from the same
245 condition (Suppl. Figure **2c**; sample with a strikethrough line). Following normalisation and quality control
246 procedures, we undertook differential methylation analysis by converting β -values to M-values (M-value =
247 $\log_2(\beta / (1 - \beta))$), as M-values show distributions that are more statistically valid for the differential analysis
248 of methylation levels⁵⁶. We undertook a 1-way ANOVA for comparisons of young and aged skeletal muscle
249 tissue. For primary human muscle cells, we undertook a 2-way ANOVA for age (young vs. aged cells) x time
250 (0, 72 h, 7 and 10 d) and also explored the ANOVA main effects for both age and time independently. We
251 also performed planned contrasts within the differentiation time-course in both young adult cells alone and
252 aged cells alone e.g. 0 h vs. 72 h, 0 h vs. 7 d 0 h vs. 10 d, as well as planned contrasts for young vs aged cells
253 at each time point of differentiation (0 h vs. 0 h, 72 h vs. 72 h, 7 d vs. 7 d, 10 d vs. 10 d in aged vs. young adult

254 cells respectively). Any CpG with a False Discovery Rate (FDR) ≤ 0.05 was deemed significant. In some
255 analyses, e.g. $> 100,000$ differentially methylated CpG sites were identified at FDR ≤ 0.05 , so we also show
256 results at a more stringent FDR of ≤ 0.01 or 0.001 , or at FDR of ≤ 0.05 and 'a change (difference in M-value)
257 in methylation greater than 2'. These shorter lists of CpGs contain the most significant sites to enable sensible
258 pathway analysis. We specify when a more stringent FDR than 0.05 was used in the results text. We then
259 undertook CpG enrichment analysis on these differentially methylated CpG lists within gene ontology and
260 KEGG pathways^{57, 58, 59} using Partek Genomics Suite and Partek Pathway. We also undertook differentially
261 methylated region analysis (e.g. identifies where several CpGs are consistently differentially methylated
262 within a short chromosomal location/region) using the Bioconductor package DMRcate
263 (DOI: [10.18129/B9.bioc.DMRcate](https://doi.org/10.18129/B9.bioc.DMRcate)). Finally, in order to plot temporal changes in methylation across the time-
264 course of muscle cell differentiation we undertook Self Organising Map (SOM) profiling of the change in mean
265 methylation within each condition using Partek Genomics Suite.

266

267 *RNA isolation, primer design & gene expression analysis*

268 Skeletal muscle tissue muscle was homogenised in tubes containing ceramic beads (MagNA Lyser Green
269 Beads, Roche, Germany) and 1 ml Tri-Reagent (Invitrogen, Loughborough, UK) for 45 seconds at 6,000 rpm \times
270 3 (and placed on ice for 5 minutes at the end of each 45 second homogenization) using a Roche Magnalyser
271 instrument (Roche, Germany). Human cells from differentiation experiments were also lysed in 300 μ l Tri-
272 Reagent for 5 minutes at RT mechanically dissociated/lysed using a sterile scraper. RNA was then isolated as
273 per Invitrogen's manufacturer's instructions for Tri-reagent. Then a one-step RT-PCR reaction (reverse
274 transcription and PCR) was performed using QuantiFast™ SYBR Green RT-PCR one-step kits on a Rotorgene
275 3000Q. Each reaction was setup as follows; 4.75 μ l experimental sample (7.36 ng/ μ l totalling 35 ng per
276 reaction), 0.075 μ l of both forward and reverse primer of the gene of interest (100 μ M stock suspension), 0.1
277 μ l of QuantiFast RT Mix (Qiagen, Manchester, UK) and 5 μ l of QuantiFast SYBR Green RT-PCR Master Mix
278 (Qiagen, Manchester, UK). Reverse transcription was initiated with a hold at 50°C for 10 minutes (cDNA
279 synthesis) and a 5-minute hold at 95°C (transcriptase inactivation and initial denaturation), before 40-50 PCR
280 cycles of; 95°C for 10 sec (denaturation) followed by 60°C for 30 sec (annealing and extension). Primer
281 sequences for genes of interest and reference genes are included in Table 1. All genes demonstrated no
282 unintended targets via BLAST search and yielded a single peak after melt curve analysis conducted after the
283 PCR step above. All relative gene expression was quantified using the comparative Ct ($\Delta\Delta$ Ct) method⁶⁰. For
284 human cell differentiation analysis via measurement of myoD and myogenin, a pooled mean Ct for the 0 h
285 young adult control samples were used as the calibrator when comparing aged vs. young adult cells. This
286 approach demonstrated a low % variation in C_t value of 9.5 and 8.5% for myoD and myogenin, respectively.
287 For HOX gene analysis between young and aged tissue and for the 7 d aged cells vs. 7 d young adult cells, the
288 mean Ct of the young adult cells were used as the calibrator. The average, standard deviation and variations
289 in Ct value for the B2M reference gene demonstrated low variation across all samples (mean \pm SD, 13.12 \pm

290 0.98, 7.45% variation) for the analysis of myoD and myogenin. For HOX gene analysis, the RPL13a reference
291 gene variation was low in the human tissue (17.77 ± 1.71 , 9.6% variation) and stem cell (15.51 ± 0.59 , 3.82%
292 variation) experiments. The average PCR efficiencies of myoD and myogenin were comparable ($94.69 \pm 8.9\%$,
293 9.4% variation) with the reference gene B2M ($89.45 \pm 3.76\%$, 4.2% variation). The average PCR efficiencies
294 of the all genes of interest in the tissue analysis of the HOX genes were also comparable ($90.87 \pm 3.17\%$,
295 3.39% variation) with the human reference gene RPL13a ($92 \pm 2.67\%$, 2.9% variation). Similarly, for the cell
296 analysis, HOX genes of interest efficiencies were comparable ($89.59 \pm 4.41\%$, 4.93% variation 4.93%) with the
297 reference gene RPL13a ($89.57 \pm 3.55\%$, 3.97% variation). Statistical analysis for HOX genes was performed
298 using t-tests (aged tissue vs. young tissue and 7d aged versus 7d young).

299

300 *Physical Activity and DNA methylation*

301 The human association study involved 30 physically active and endurance-oriented men of Eastern European
302 descent (32.9 ± 9.9 years). The study was approved by the Ethics Committee of the Physiological Section of
303 the Russian National Committee for Biological Ethics and Ethics Committee of the Federal Research and
304 Clinical Center of Physical-chemical Medicine of the Federal Medical and Biological Agency of Russia. Written
305 informed consent was obtained from each participant. The study complied with the guidelines set out in the
306 Declaration of Helsinki. Physical activity was assessed using questionnaire. Participants were classified as
307 mildly active (1-2 training sessions per week, n=6), moderately active (3-4 training sessions per week, n=8)
308 and highly active (5-7 sessions per week, n=16) participating in aerobic exercise for at least the last 6 months.
309 Bisulfite conversion of genomic DNA was performed using the EpiMark® Bisulfite Conversion Kit in
310 accordance with the manufacturer's instructions. In the same analysis as described above for the aged muscle
311 tissue and stem cell data, methylome of the vastus lateralis in the physically active men was evaluated using
312 the Infinium MethylationEPIC 850K BeadChip Array (Illumina, USA) and imaged and scanned using the
313 Illumina iScan® System (Illumina, United States). Also as in the above analysis we filtered out probes located
314 in known single-nucleotide polymorphisms (SNPs) and any known cross-reactive probes using previously
315 defined SNP and cross-reactive probe lists⁶¹. Low quality probes were also filtered, as with the above
316 analysis. The final analyses included 796,180 of 868,565 probes. Data were normalised using the same
317 functional normalisation (with noob background correction), as in the aged tissue and stem cell data, and as
318 previously described⁵⁵. Any outliers were interrogated via PCA as above, however all samples passed the QC
319 and therefore there were no outliers. The methylation level of each CpG-site after normalization and filtering
320 processes was represented as a β -value ranging from 0 (unmethylated) to 1 (fully methylated) in order to
321 undertake multiple regression (as regression analysis performed better with finite values. Ideally, if values
322 range from 0 to 1 with beta-values satisfying this criteria). Statistical analyses were conducted using PLINK
323 v1.90, R (version 3.4.3) and GraphPad InStat (GraphPad Software, Inc., USA) software. Multiple regression
324 was used for testing associations between the CpG-methylation level and physical activity adjusted for age
325 and muscle fibre composition. With methylation level as the dependent variable, and physical activity and

326 age as independent variables. P values < 0.05 were considered statistically significant to test the identified
327 HOX CpG sites. The p value is given for the physical activity score adjusted for age and muscle fibre
328 composition.

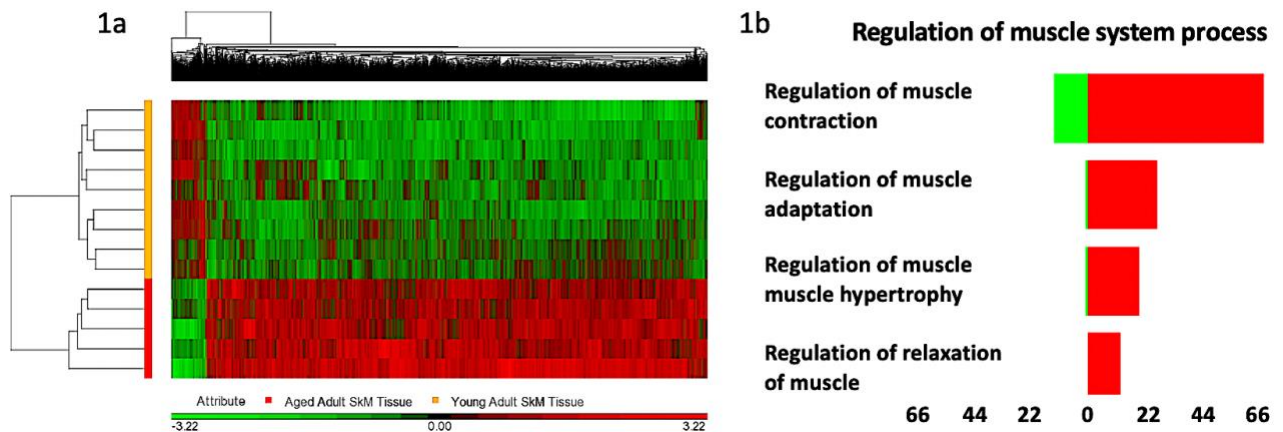
329

330 **Results**

331

332 *Aged human skeletal muscle tissue is hypermethylated compared with young adult tissue*

333 There were 17,994 differentially methylated CpG positions (DMPs) between aged and young adult tissue at
334 FDR \leq 0.05 (Suppl. File **1a**), and 6,828 DMPs at a more stringent FDR of \leq 0.01 (Suppl. File **1b**). The
335 overwhelming majority of the 6,828 DMPs (93%) were hypermethylated in aged compared with young
336 muscle (Figure **1a**). Furthermore, DMPs were enriched in CpG islands (5,018 out of 6,828 CpG's) with the
337 remaining in N-shores (354), S-Shelf (48), S-Shores (341), S-Shelf (69) and 'other' (998). Ninety nine percent
338 of the DMPs (4,976 out of the 5,018 CpGs) located in CpG islands were also hypermethylated with age
339 compared to young adult tissue (Suppl. File **1c**). After gene ontology analysis on these DMPs (Suppl. File **1d**),
340 hypermethylation was enriched within the three overarching gene ontology terms: 'Biological process'
341 (Suppl. Figure **3a**), 'cellular component;' (Suppl. Figure **3b**), and 'molecular function' (Suppl. Figure **3c**). Within
342 the GO terms that included the search term 'muscle', the most significantly enriched was 'regulation of
343 muscle system process' (Figure **1b**, CpG list Suppl. File **1e**). Within this GO term was 'regulation of muscle
344 contraction' (CpG list Suppl. file **1f**). Further, we found hypermethylation enrichment in KEGG pathways:
345 'Pathways in cancer', 'Rap1 signaling', 'Axon guidance' and 'Hippo signaling' (Suppl. File **1g**). Within the top
346 enriched pathway, 'pathways in cancer', 96% (266 out of 277 CpGs) were hypermethylated and only the 4%
347 (11 CpGs) were hypomethylated in aged compared with young adult muscle tissue (Suppl. Figure **4**; Suppl.
348 File **1h**). Differentially methylated regions (DMRs) were also analysed between young and aged skeletal
349 muscle tissue (Suppl. File **1i**). The top 5 DMRs were identified as: chr8:22422678-22423092 (415 bp) within a
350 CpG island of the SORBS3 gene with 6 CpG's that were all hypermethylated in aged versus young adult tissue.
351 Also, chr6:30653732-30655720 (1989 bp) within a CpG island of the PPPR1 gene contained 8 CpG's that were
352 all hypermethylated compared with young adult muscle. Chr20:13200939-13202437 (1499 bp) within a CpG
353 island of the promoter of gene ISM, contained 8 CpG sites were also all hypermethylated. Similarly, the gene
354 PDE4D1P on Chr1:144931376-144932480 (1105 bp) contained 6 CpG sites that spanned its promoter within
355 a CpG island, once again demonstrating hypermethylation. The only gene demonstrating the opposite
356 direction in methylation status (hypomethylation) in aged tissue was the gene C1orf132 (new gene name
357 MIR29B2CHG), also on chromosome 1 (Chr1:207990896-207991936; 1041 bp), where 5 CpGs within this
358 region were hypomethylated in opposition to the majority of gene regions that were hypermethylated in
359 aged versus young tissue.



360

361

362

363

364

365

366

367

368

369

370

371

372

373

374

375

376

377

378

379

380

381

382

383

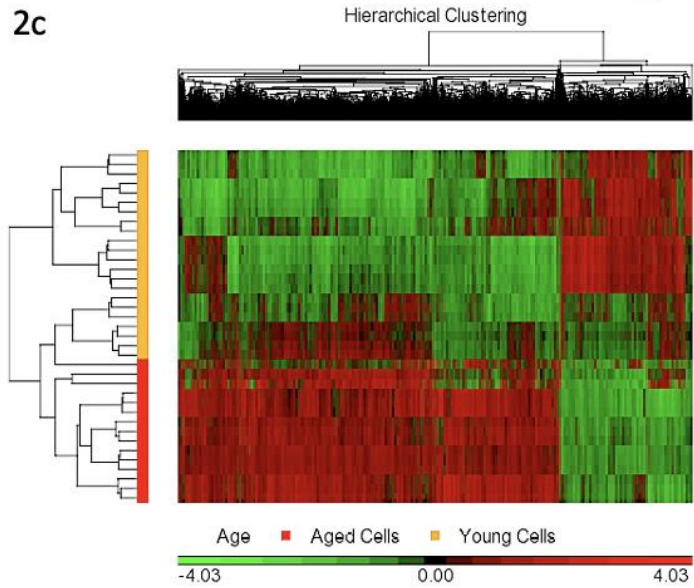
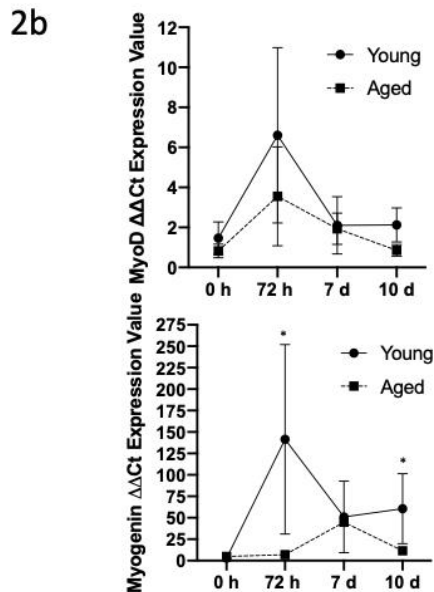
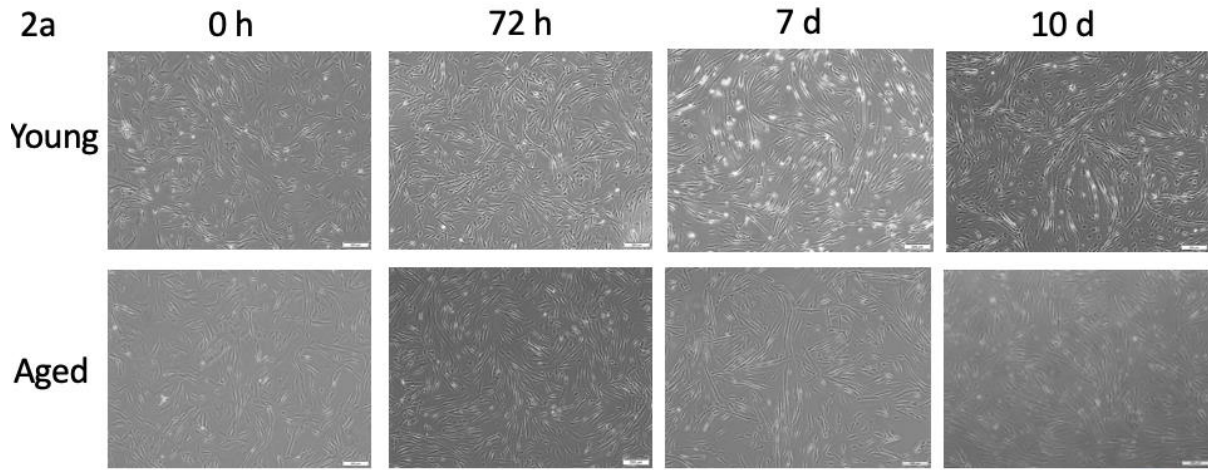
384

385

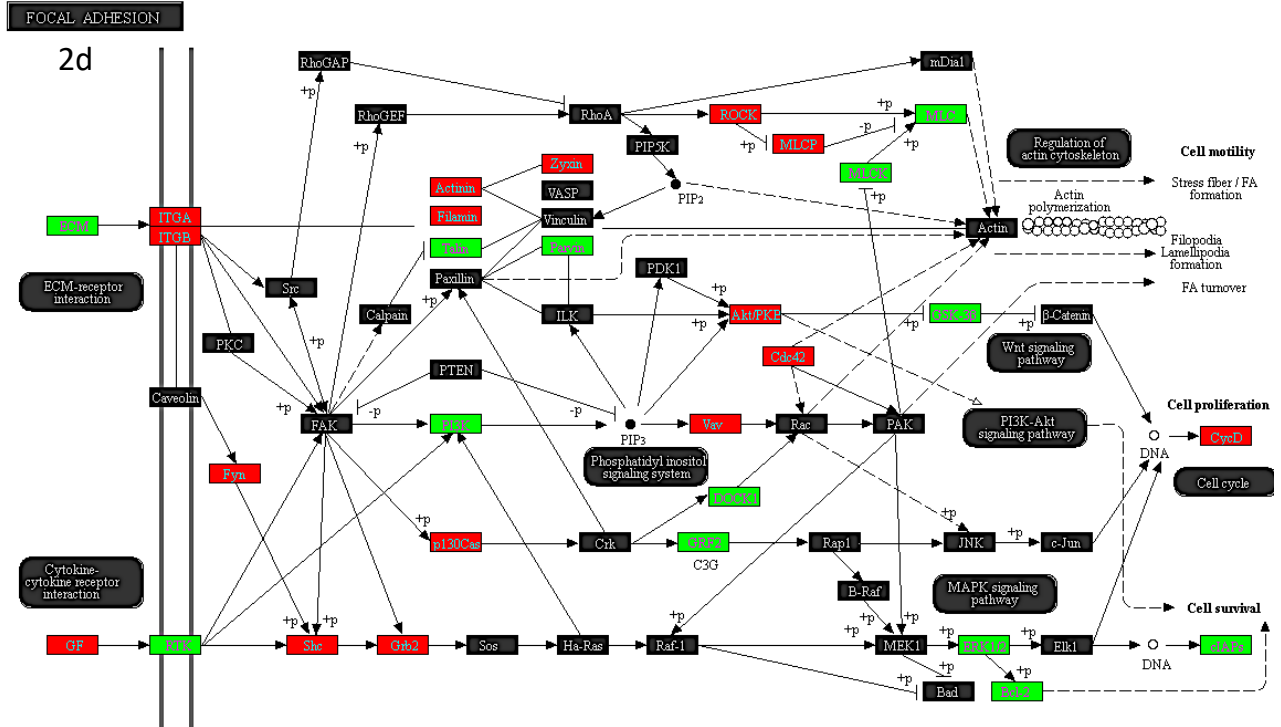
Figure 1. DNA methylation across the genome in aged human skeletal muscle tissue compared with young adult tissue. 1a. Hierarchical clustering heatmap of the significantly differentially methylated CpG sites, depicting aged skeletal muscle containing a hypermethylated (RED) versus hypomethylated (GREEN) signature compared with young adult tissue. **1b.** Significantly enriched CpG sites for most significantly enriched GO term containing the search term ‘muscle’; ‘regulation of muscle system process’ (RED hypermethylated and GREEN hypomethylated CpGs).

Aged primary human muscle stem cells displayed more varied DNA methylation signatures versus young adults during the time-course of differentiation

We analysed DNA methylation from differentiating human muscle stem cells at 0 h (30 minutes post dropping to 2% serum), 72 h, 7 and 10 d. Both young and aged adult cells demonstrated morphological differentiation and myotube formation as the cells advanced across the time-course (Figure **2a**). This was confirmed by increases in myoD and myogenin mRNA expression in both young and aged cells as differentiation progressed up to 72hrs (Figure **2b**). However, myotube formation was less extensive in elderly cells, despite young and aged cells having identical numbers of starting myogenic cells. This age associated reduction in differentiation was confirmed with significantly reduced myoD and myogenin gene expression at 72 h and 10 d ($p \leq 0.05$), as well as by delayed increases in myogenin mRNA expression (Figure **2b**) in aged cells. A similar delay has been shown previously to be associated with impairing the fusion process and myotube formation^{32,33}. There were also differences in DNA methylation between aged and young cells during differentiation. Indeed, the interaction for a 2-way ANOVA (Age \times Time) generated a list of 40,854 CpG sites that were significantly altered with age and across the time-course of differentiation (FDR ≤ 0.05 , Suppl. File **2a**). With a more stringent FDR ≤ 0.01 and ≤ 0.001 there were still 9,938 and 2,020 CpG’s significantly differentially methylated respectively in aged cells versus young cells across all time points of differentiation (Suppl. File **2b** and **2c** respectively).



386



387

388

389

Figure 2. Aged and young adult primary muscle derived stem cells differentiated over 0, 72 h, 7d and 10 d and differences in DNA methylation. a. Light microscope images of aged versus young muscle derived stem cells, depict fewer myotubes in aged versus

390 young cells, particularly at 7 and 10 days. **b.** MyoD and myogenin gene expression in aged versus young cells over the differentiation
391 time course. Where, reductions in myogenin were observed at 72 h in aged cells as well as a delayed increase in the upregulation of
392 myogenin compared with young cells. **c.** Hierarchical clustering heatmap of the significantly differentially methylated CpG sites
393 between aged and young muscle stem cells across the entire time-course of differentiation (all time points of 0, 72 h, 7 d and 10 d).
394 RED hypermethylated and GREEN hypomethylated. **d.** Comparison of DNA methylation in aged versus young muscle stem cells at 7
395 d of differentiation (7 d aged vs. 7 d young adult cells) in most enriched KEGG pathway, 'focal adhesion'. Note, because some genes
396 have multiple CpGs per gene, Partek Pathway (Partek Genomics Suite) used to create figure 2d, selects the CpG with the lowest p-
397 value (most significant) and uses the beta-value for that particular CpG to colour the pathway diagram. This is therefore accurate in
398 situations where CpGs on the same gene have the same methylation pattern (e.g. all hyper or hypomethylated). However, where
399 multiple CpGs on the same gene have the different methylation pattern (e.g. some hypomethylated and others hypermethylated),
400 only the most significant methylated CpG is chosen and represented in the image. For full and accurate significant CpG lists, including
401 the sites that were hypo and hypermethylated in this 'focal adhesion' pathway, are included in Suppl. File 5i.
402

403 We next assessed changes in DNA methylation across time during differentiation (main effect for 'time') i.e.
404 changes in DNA methylation overtime time that was visible in both young and old cells). However, we did
405 not find time-related DMPs at our statistical cut off of $FDR \leq 0.05$. This suggested, that DNA methylation was
406 not considerably changing over the time course of muscle stem cell differentiation itself. We therefore
407 contrasted each timepoint of differentiation with the baseline (0 h timepoint) in young and aged cells to
408 further examine this observation. Indeed, in young adult cells, there were only 1 and 14 DMPs at 72 h and 10
409 d respectively ($FDR \leq 0.05$), and no DMPs at 7 d ($FDR \leq 0.05$) compared to their baseline 0 h timepoint. In
410 aged cells, there were no DMPs during early differentiation (72 h vs. 0 h, $FDR \leq 0.05$) but 2,785 significant
411 DMPs at 7 days of differentiation (7d vs. 0 h, $FDR \leq 0.05$, Suppl. file **2d**) and 404 DMPs at 10 days of
412 differentiation (10 d vs. 0 h, $FDR \leq 0.05$, Suppl. File **2e**). Therefore, while the differentiation itself was not
413 changing DMPs in young cells there were a significant number of DMPs at 7 days of differentiation in aged
414 cells compared with their own 0 h timepoint. Using more stringent cut-offs ($FDR \leq 0.05$ and
415 change/difference in methylation greater than 2), at this 7-day time point in aged cells there were 1,229
416 DMPs at 7 d vs 0 h (Suppl. File **2f**), with a balanced number of hypo and hypermethylated DMPs. Overall, this
417 may suggest a more dysfunctional DNA methylation program during differentiation in aged human muscle
418 cells compared with young cells. Conducting gene ontology analyses at this 7 day time point (Suppl. File **2g**),
419 it suggested that this varied methylation response in aged cells was enriched in GO terms: 'regulation of
420 localisation', 'regulation of cell communication' and 'regulation of signaling' (Suppl. Figure **5**; Suppl. File **2h**,
421 **i**, **j** respectively). CpGs within these ontologies also confirmed that there was a similar hypo and
422 hypermethylation profile in aged cells at 7 days. Further, KEGG pathway analysis suggested the top enriched
423 pathways at 7 days in aged cells versus 0 h were: 'axon guidance', 'cholinergic synapse', 'adrenergic signaling
424 in cardiomyocytes' and 'circadian entrainment' (Suppl. File **2k**). Finally, DMR analysis between young and
425 aged cells at 7 days of differentiation identified two regions in 2 genes that had 5 or more CpG sites
426 significantly differentially methylated (Suppl. File **2l**). The first being Chr3:155394096-155394303 (209 bp)
427 located on gene PLCH1 that had 5 of its CpG's hypomethylated. The second being a region non-annotated in

428 location Chr2: 119615888-119617128 (1241 bp) that was hypermethylated on 5 CpG's. Suggesting that
429 enriched and varied methylation of these regions occurred at 7 d differentiation in aged cells that was not
430 detected at 7 days in young adult cells.

431

432 *Aged muscle cells demonstrate hypermethylated signatures versus young muscle cells across differentiation,*
433 *particularly at 7 days*

434 We next wished to identify differences in DNA methylation in aged versus young muscle stem cells. The main
435 effect for 'age' generated a significant differentially methylated (FDR \leq 0.05) CpG list of 269,898 sites that
436 significantly varied in aged cells versus young cells. Even with a more stringent cut-off (FDR \leq 0.01) there
437 were still 159,235 sites significantly modified (Suppl. File **3a**). Increasing the stringency to a difference of
438 greater than 2 while keeping an FDR \leq 0.01 identified 2,719 DMPs with the most highly significant and
439 demonstrated the largest differences between aged and young cells (Suppl. File **3b**). As with the aged versus
440 young skeletal muscle tissue analysis, the majority of these significantly modified CpG sites in aged cells were
441 hypermethylated (2,017 out of 2,719) versus hypomethylated (702 out of 2,719) compared with young cells,
442 visualised in hierarchical clustering aged cells vs. young cells (Figure **2c**). Two hundred and eleven out of these
443 2,719 CpGs were located in islands and 97 were promoter associated. Gene ontology identified that aged
444 cells demonstrated this significantly enriched hypermethylated profile in GO terms: 'developmental process',
445 'anatomical structure development', 'anatomical structure morphogenesis' (Suppl. File **3c**) and also in KEGG
446 pathways 'axon guidance', 'adherens junction', 'calcium signaling', 'focal adhesion' and 'protein digestion and
447 absorption' (Suppl. File **3d**). DMR analysis (Suppl. File **3e**) identified that a non-coding location on
448 chr12:115134344-115135576 (1233 bp) that contained 13 CpG's that were hypermethylated in aged cells
449 versus young cells. Further, there were 7 CpG's that were hypermethylated in the region of the gene LY6G5C
450 (Chr6:31650736-31651158, 423 bp). There was also region containing 8 CpGs of the HOXC10 gene just
451 upstream of HOXC6 and MIR196 (Chr12:54383692-54385621, 1933 bp) that all demonstrated a
452 hypomethylated profile in aged cells vs. young cells. Interestingly, on the same chromosome just upstream
453 of the HOXC10 gene (Chr12:54376020-54377868, 1849 bp), within the lncRNA HOXC-AS3, there were
454 another 6 CpGs that were hypomethylated in aged cells versus young cells. The concentration of
455 hypomethylated CpGs in aged versus young cells in HOXC genes is interesting given the majority of CpG's,
456 more generally, were hypermethylated in aged cells versus young cells. A finding that is taken further in the
457 later results section below.

458

459 Given these changes, predominantly favouring hypermethylation (except the HOXC genes identified above)
460 in aged cells versus young cells, we also performed contrasts between aged and young adult cells at each
461 time point of differentiation. When we compared 0 h aged cells with young adult cells at 0 h, we identified
462 738 DMPs between young and old cells (FDR \leq 0.05, with a difference/change greater than 2), 79% of which
463 were hypermethylated in aged versus young cells (Suppl. File **3f**). Gene ontology analysis (Suppl. File **3g**)

464 revealed that the DMPs were in genes enriched for ‘cytoskeletal protein binding’ (Suppl. Figure **6a**; Suppl.
465 File **3h**), ‘developmental process’, ‘cell junction’, ‘cytoskeleton’ and ‘actin binding’ (Suppl. File **3i, j, k, l**
466 respectively). KEGG pathway analysis of 0 h aged versus 0 hr young adult cells (Suppl. File **3m**) also suggested
467 that there were significantly enriched hypermethylated pathways for ‘Axon Guidance’ (Suppl. Figure **6b**; CpG
468 List Suppl. File **3n**), ‘Insulin secretion’, ‘Phospholipase D signaling’, ‘cAMP signaling pathway’ and
469 ‘Aldosterone synthesis and secretion’ (Suppl. Files **3o, p, q, r** respectively). At 72 h d, there were 1,418 DMPs
470 between aged and young adult cells ($FDR \leq 0.05$), and with a difference/change greater than 2 there were
471 645 significant CpG sites between aged and young adult cells (Suppl. File **4a**), 74% of which were
472 hypermethylated in aged vs. young cells. Gene ontology analysis (Suppl. File **4b**) revealed that the DMPs were
473 in genes enriched for ‘cytoskeletal protein binding’ (Suppl. Figure **6c**; Suppl. File **4c**), ‘actin binding’ (Suppl.
474 File **4d**), ‘cytoskeleton’ and ‘development process’ as most significantly enriched, followed by ‘regulation of
475 signaling’ (Suppl. Files **4e, f, g** respectively). KEGG pathway analysis (Suppl. File **4h**) showed enrichment for
476 ‘Insulin secretion’ (Suppl. File **4i**), ‘aldosterone synthesis and secretion’ (Suppl. File **4j**) and ‘cAMP signaling
477 pathway’ (Suppl. Figure **6d**, Suppl. Files **4k**).

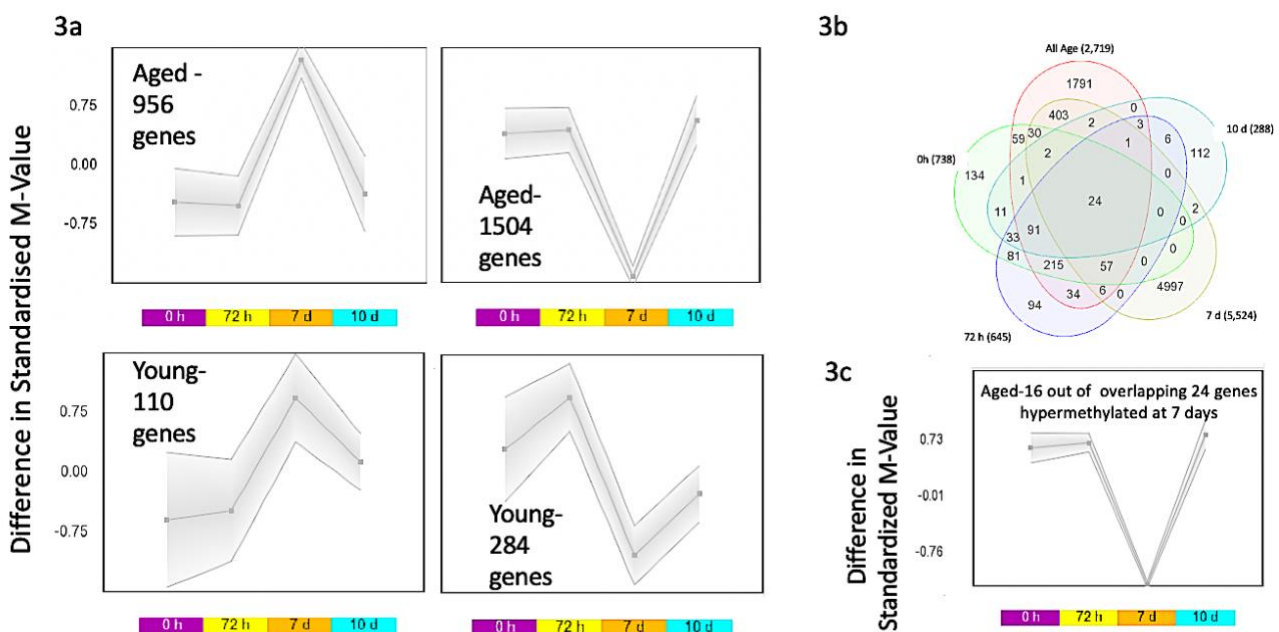
478
479 It was at 7 d of differentiation that we identified the largest number of DMPs between young and old cells
480 (5,524 DMPs at $FDR \leq 0.05$, with a difference/change greater than 2, Suppl. File **5a**). 74% of DMPs were
481 hypermethylated in aged vs. young cells. Gene ontology analysis (Suppl. File **5b**) revealed that DMPs were in
482 genes enriched for ‘developmental process’ (Suppl. Figure **7a**, Suppl. File. **5c**) ‘anatomical structure
483 morphogenesis’ (Suppl. File **5d**), ‘neuron part’, ‘cytoskeletal protein binding’ and ‘cell junction’ (Suppl. File **5**
484 **e, f, g**). KEGG analysis (Suppl. File **5h**) identified: ‘Focal adhesion’ (Figure **2d**; Suppl. file **5i**), ‘adherens junction’
485 (Suppl. File **5j**), ‘regulation of actin cytoskeleton’ (Suppl. File **5k**), ‘cGMP-PKG signaling pathway’ Suppl. File
486 **5l**), ‘rap1 signaling pathway’ (Suppl. File **5m**), as well as the muscle differentiation pathway of ‘PI3K-Akt
487 signaling pathway’ (Suppl. Figure **7b**, Suppl. File **5n**). Among the DMRs at 7 d (Suppl. File **5o**) was a region
488 within *HOXB1*, containing 8 hypermethylated CpGs in aged vs. young cells. We also identified to be
489 hypermethylated in differentiation in aging cells only at 7 days, the gene LY6G5C, this time spanning a slightly
490 larger region Chr6:31650736-31651362, of 627 bp (vs. Chr6:31650736-31651158, 423 bp in the above
491 analysis), confirming that 6 of its CpG’s were hypermethylated at 7 d compared with young adult cells at the
492 same time point. At 10 d, we identified 288 DMPs ($FDR \leq 0.05$ with a change greater than 2, Suppl. File **6a**),
493 89% of which were hypermethylated in aged vs. young cells. Gene ontology analysis (Suppl. File **6b**) revealed
494 that the DMPs were in genes enriched for ‘GDP binding’ (Suppl. Figure **7c**, Suppl. File **6c**), ‘phosphotransferase
495 activity’, ‘positive regulation of antigen receptor’, ‘mesoderm morphogenesis’ and ‘actin binding’ (Suppl. File
496 **6d, e, f, g** respectively). KEGG analysis (Suppl. File **6h**) identified ‘Regulation of actin cytoskeleton’ (Suppl.
497 Figure **7d**; Suppl. File **6i**), ‘ErbB signaling pathway’ (Suppl. File **6j**) and ‘Selenocompound metabolism’ (Suppl.
498 File **6k**).

499

500 *Self-organising map (SOM) profiling of aged muscle stem cells confirm a varied methylation profile in aged*
 501 *cells compared with young cells*

502 In order to further analyse temporal dynamics in methylation over the time course of differentiation in aged
 503 versus young cells, we conducted SOM profiling analysis of the 2,719 DMPs generated above (Suppl. File **3b**
 504 above, those highly significant for 'age'). SOM analysis averages the methylation values for the group of
 505 samples within each condition to identify temporal profile changes in DMPs between aged and young cells
 506 over the time-course of differentiation. Aged cells demonstrated more varied DNA methylation changes
 507 earlier in the time-course of differentiation (between 72 h and 7 d) compared with young adult cells (Figure
 508 **3a**). When looking at aged cells temporal dynamics compared with young cells, out of the 2,719 DMPs in
 509 aged cells 1,504 were hypomethylated and 956 hypermethylated at 7 days (confirming the aged cells 'time'
 510 main effect analysis above). With only a small number of genes demonstrating this altered profile at 7 days
 511 in young cells (284 hypomethylated and 110 hypermethylated out of the 2,719 CpG list).

512
 513 Finally, in order to identify common CpG changes between aged and young cells at each time point, the
 514 significantly differentially methylated DMPs from young vs. aged cells across all time were overlapped (2,719
 515 CpG list), with the 0 h aged vs. 0 h young (738 CpG list), 72 h aged vs. young 72 h (645 CpG list), 7 d aged vs.
 516 7 d young (5,524 CpG list), and the 10 d aged vs 10d young (288 CpG list) (Venn diagram, Figure **3b**). There
 517 were 24 genes that were identified across tissue and stem cell analysis that were significantly differentially
 518 methylated (Suppl. File **7a**). They included 24 CpG's on 16 genes: TSPAN9, RBM22, UBAP1, CAPZB, ZNF549,
 519 MBNL2, RMI1, CHRM5, RAB4A, C19orf21, MOBKL1A, ANAPC11, GAS7, PBX1, ELOVL2, FGGY. Furthermore,
 520 generating a SOM profile of temporal change in methylation over the time-course of differentiation in these
 521 24 CpG's, (Figure **3c**), also demonstrated that the majority of these DMPs in aged cells (16 out of 24 CpG's)
 522 demonstrated varied methylation at 7 days (11 out of 16 CpGs on annotated genes: TSPAN9, RBM22, UBAP1,
 523 CHRM5, C19orf21, ELOVL2, MOBKL1A, ANAPC11, PBX1, CAPZB, FGGY; fully detailed in Suppl. File **7a**).



524

525 **Figure 3. SOM profiling of DNA methylation over the time-course of differentiation in aged versus young adult muscle stem cells.**
526 **a.** Demonstrates a larger number of hypomethylated and hypermethylated CpG sites in aged muscle stem cells, particularly at 7 days
527 of differentiation, compared with young adult muscle stem cells. **b.** Venn Diagram analysis depicting the 24 common CpG sites that
528 were altered at every time point of differentiation between aged and young adult muscle stem cells (0, 72 h, 7d and 10 d). **c.** As with
529 the above analysis in 3a, SOM profiling identified that 16 out of these 24 CpG's also demonstrated the most varied methylation
530 dynamics at 7 days of differentiation in aged cells.

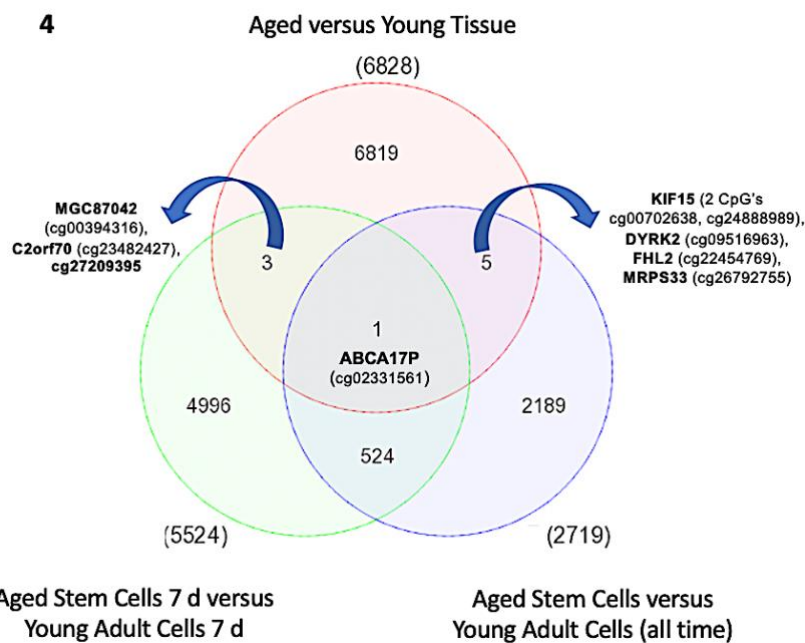
531
532 *Distinguishing differentiation-specific CpG sites in aged cells versus those altered as a consequence of age*
533 *alone*

534 The data above suggest that aged cells demonstrate hypermethylation versus young adult cells across all
535 stages of differentiation, and that aged cells significantly altered their methylation profiles at 7 days of
536 differentiation. Therefore, we conducted further analysis on the overlap of DMPs within aged cells at 7 d of
537 differentiation (from the 'time' analysis above) and those that were changed as a consequence of age at 7
538 days (aged cells at 7 days versus young cells at 7 d). This enabled the identification of which methylation sites
539 were altered, but also shared in both aged cell differentiation alone and as a consequence of age. Or,
540 alternatively the sites that were simply changed with age and not differentiation process and vice versa.
541 Indeed, overlapping the aged cells 0 h vs. 7 d (1,229 DMP list) with the 7 d young cells significant 5,524 DMP
542 list, there were only 334 (206 hypermethylated, 128 hypomethylated) DMPs that were shared (Suppl. File.
543 **8a**). This suggested that differentiation itself modified only 334 DMPs (out of 1,229) in aged cells that were
544 also changed as a consequence of age (i.e. in aged vs. young cells at 7 days). The remaining 895 DMPs (1,229
545 - 334 DMPs; Suppl. File **8b**) were differentiation specific to aged cells. Out of this 895 DMP list, an equal
546 number were hypo and hypermethylated (458 hypo and 437 hypermethylated). Therefore, this overlap
547 analysis also confirmed that data above, where over the time-course of aged cell differentiation itself the
548 methylome is both hypo and hyper methylated on a similar number of DMPs, whereas aging alone
549 predominantly hypermethylates (where out of 5,524 changed at 7 d young vs. aged, 4061 were
550 hypermethylated and only 1,463 hypomethylated). This also suggested that the remaining 5,190 (5,524
551 minus 334 DMP list, equalling 5,190 DMPs including 3,910 hypermethylated vs. 1,280 hypomethylated) were
552 as a consequence of aging alone (Suppl. File **8c**).

553
554 *Hypermethylation for a small number of CpG sites is similarly altered in aged muscle cells in-vitro from the in-*
555 *vivo tissue niche.*

556 Tissue and cell PCA plots demonstrated that methylation of even late differentiated cells was vastly different
557 to tissue, suggesting that cell versus tissue samples were comprised of vastly different methylation profiles
558 (Suppl. Figure **8**). Therefore, in order to compare if there were any sites similarly altered in the cells that were
559 also altered in the tissue with age, we overlapped the DMP lists from the tissue and cell analysis described
560 above. Six CpG's that were identified in the 6,828 significantly differentially methylated CpG list from the
561 aged versus young tissue analysis, as well as highlighted in the 2,719 list 'age' cells analysis (Figure **4**). These

562 included: KIF15 (2 CpG's Cg00702638 & cg24888989), DYRK2 (cg09516963), FHL2 (cg22454769), MRPS33
 563 (cg26792755), ABCA17P (cg02331561). All of these genes were hypermethylated in the tissue analysis as well
 564 as the cells. Given that aged cells demonstrated the most varied methylation at 7 days versus young cells.
 565 When comparing 7 d aged vs. 7 d young cell list (5,524 list), 4 CpG's (out of the 6 CpG sites identified above)
 566 were also identified in the 6,828 tissue CpG list, including: MGC87042 (cg00394316), C2orf70 (cg23482427),
 567 ABCA17P (cg02331561) and cg27209395 (not on an annotated gene). Once more, all of these CpG's (with the
 568 exception of C2orf70, cg23482427) were hypermethylated in the tissue analysis as well as the cells. With
 569 ABCA17P (cg02331561) highlighted across all gene lists (**Figure 4**).

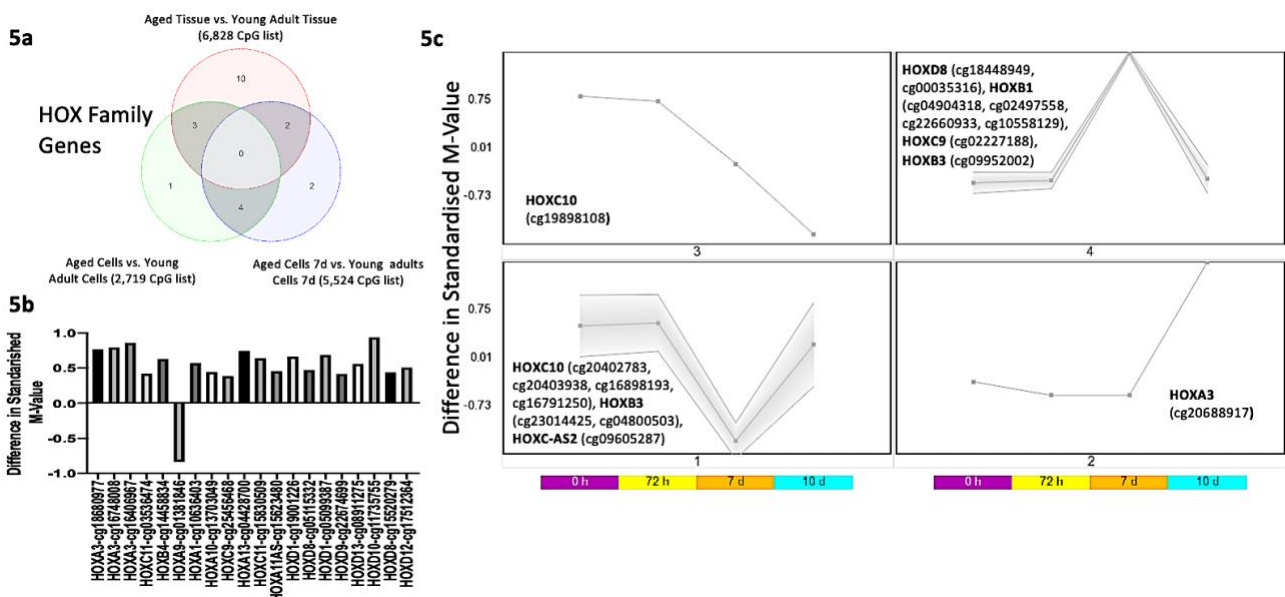


586 (cg00394316), C2orf70 (cg23482427), ABCA17P (cg02331561) and cg27209395 (not on an annotated gene). Once more, all of these
 587 CpG's (with the exception of C2orf70, cg23482427) were hypermethylated in the tissue analysis as well as the stem cells. With
 588 ABCA17P (cg02331561) highlighted across all CpG lists.

589
 590 *Varied methylation in the HOX family of genes in aging skeletal muscle tissue and stem cells*

591 In the above analyses in aged versus young cells (all time points) there were 8 CpG's with altered methylation
 592 within the region of the HOXC10 gene just upstream of HOXC6 and MIR196 (Chr12:54383692-54385621,
 593 1933 bp). Also, on the same chromosome just upstream of the HOXC10 gene (Chr12:54376020-54377868,
 594 1849 bp) within lncRNA HOXC-AS3 there were another 6 CpG's that were altered in aged cells versus young
 595 cells. Similarly, within the 5,524 DMP list at 7 d in aged cells versus 7 d young adult cells (Suppl. File 5o), the
 596 time point most affected by age in the cell analysis, we also identified that a region of the HOXB1, located in
 597 Chr17:46607104-46608568 that contained 8 CpG's that were hypermethylated within the 1465 bp region.
 598 Therefore, we further analysed all the HOX gene changes in the significantly differentially methylated aged
 599 vs. young tissue (6,828 DMP list) and identified that CpG's within HOXD10, HOXD9, HOXD8, HOXA3, HOXC9,
 600 HOXB1, HOXB3, HOXC-AS2 and HOXC10 were significantly differentially methylated across all analyses,

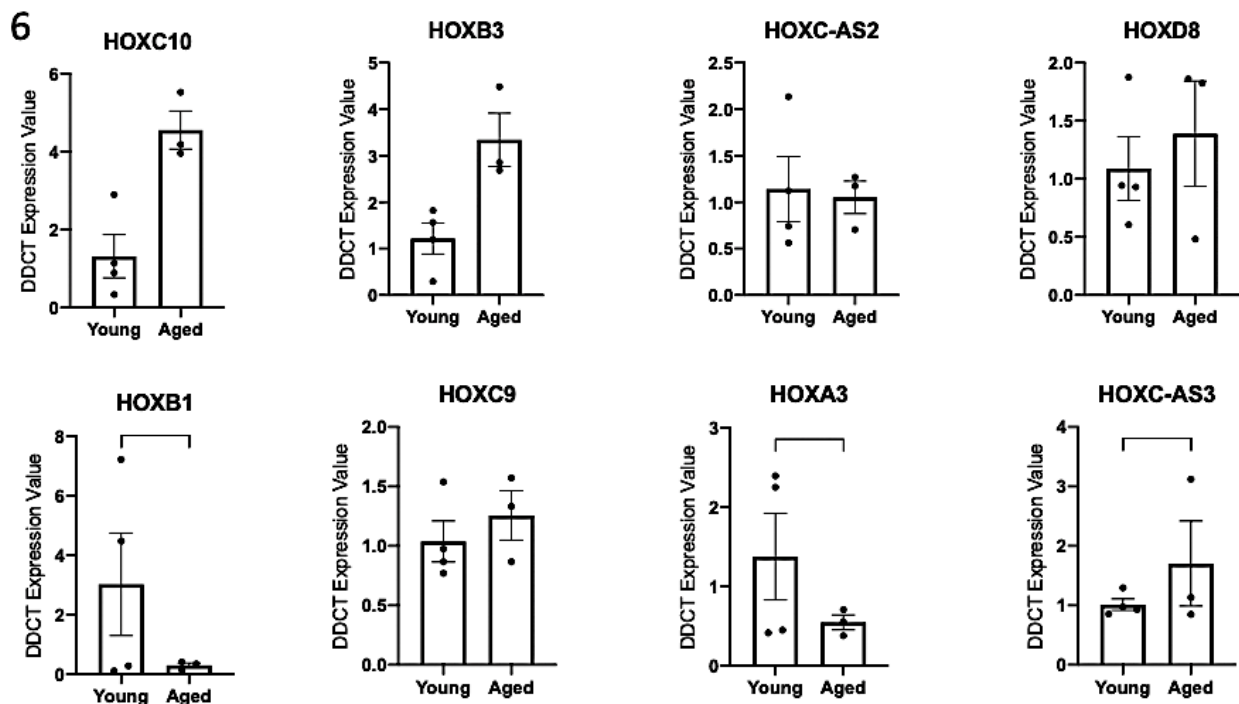
601 including the aged vs. young tissue (6,828 DMP list; Suppl. File **9a**), aged versus young adult cells (all time)
 602 2,719 DMP list (Suppl. File **9b**) as well as the 7 d aged versus 7 d young cell analysis 5,524 DMP list (Suppl.
 603 File **9c**). A Venn diagram analysis depicted the overlap in common gene symbols for these three gene lists
 604 (Figure **5a**, Suppl. File **9d**). It was also demonstrated that the majority of these HOX genes were
 605 hypermethylated in aged tissue (Figure **5b**; Suppl. File. **9a**). In the cell analysis across all time, these HOX
 606 genes also displayed the most varied methylation at 7 days of differentiation in aged cells versus young cells,
 607 therefore confirming the varied temporal profile in methylation described above at 7 d was also the case for
 608 these HOX genes. Finally, when SOM-profiling these 9 HOX genes by symbol (17 CpGs as some HOX genes
 609 contained more than one CpG site), over the time-course of differentiation based on the main effect for ‘age’
 610 2,719 significantly differentially methylated CpG list. Eight CpG sites across HOX family genes: HOXD8
 611 (cg18448949, cg00035316), HOXB1 (cg04904318, cg02497558, cg22660933, cg10558129), HOXC9
 612 (cg02227188) and HOXB3 (cg09952002) were hypermethylated at 7 days, whereas and 7 CpGs across
 613 HOXC10 (cg20402783, cg20403938, cg16898193, cg16791250), HOXB3 (cg23014425, cg04800503), HOXC-
 614 AS2 (cg09605287) were hypomethylated at 7 days (Figure **5c**; Suppl. File **9e**). This meant distinct genes were
 615 hypermethylated (HOXD8, HOXC9, HOXB1) and hypomethylated (HOXC10, HOXC-AS2) at 7 days in aged cells
 616 versus young adult cells, except for one of these genes, HOXB3, that contained 1 CpG that was
 617 hypermethylated versus 2 that were hypomethylated.
 618



619 **Figure 5. HOX family of genes and their DNA methylation in aged tissue and muscle stem cells.** a. Venn diagram identifying 9
 620 commonly differentially methylated HOX genes: including HOXD10, HOXD9, HOXD8, HOXA3, HOXC9, HOXB1, HOXB3, HOXC-AS2 and
 621 HOXC10 (note this Venn diagram analysis is by ‘gene symbol’ not ‘probe cg’ (CpG site), as some HOX genes also had more than 1 CpG
 622 per gene symbol, full CpG lists are located in Suppl. Figure **9 a,b,c,d**). b. All HOX family genes by CpG site (cg probe) differentially
 623 methylated in aged compared with young skeletal muscle tissue, predominantly all demonstrating hypermethylation. c. SOM profiling
 624 depicting the temporal regulation of DNA methylation in aged muscle stem cells as they differentiate in CpGs located amongst the
 625 HOX family of genes (depicting the 9 HOX genes altered, by gene symbol, in both the tissue and cells). The majority of these HOX CpG
 626 sites were differentially methylated at 7 days of differentiation in the aged cells.
 627

628

629 We next analysed the gene expression of the HOX genes that changed at the methylation level in both the
630 tissue and cell analysis (by gene symbol- HOXD8, HOXA3, HOXC9, HOXB1, HOXB3, HOXC-AS2 and HOXC10).
631 Interestingly, in aged tissue, despite displaying hypermethylation in all these HOX genes versus young tissue,
632 the genes were not suppressed at the gene expression level, which may have been expected, yet all elevated
633 (Suppl. Figure 9). However, in the aged cells when analysing these genes at the expression level at 7 days of
634 differentiation (including HOXD8, HOXA3, HOXC9, HOXB1, HOXB3, HOXC-AS2 and HOXC10, as well as HOXC-
635 AS3 identified in the above in the cell analysis only) (Figure 6), we identified that there was significantly
636 reduced gene expression in gene HOXB1 (Figure 6), that was inversely related with increased HOXB1
637 methylation. Where in the 5,524 DMP list at 7 d in aged cells versus 7 d young adult cells (Suppl. File 5o), we
638 previously identified that a region of the HOXB1 located in Chr17:46607104-46608568, contained 8 CpG's
639 that were hypermethylated, as well as HOXB1 Cg's: cg04904318, cg02497558, cg22660933, cg10558129
640 being identified as hypermethylated in the 2,719 significant main effect for 'age' cell CpG list above (Suppl.
641 File 3b). There was also significantly increased gene expression for HOXC-AS3, with this gene identified
642 earlier in the analysis as being having reduced (hypo)methylation. Indeed, hypomethylation occurred in 6
643 CpG's in a region upstream of the HOXC10 gene (Chr12:54376020-54377868, 1849 bp) within the HOXC-AS3
644 gene. Interestingly, HOXC10 also demonstrated an average increase in gene expression, however, it was not
645 statistically significant (Figure 6). Finally, HOXA3 also demonstrated significantly reduced expression (Figure
646 6) with corresponding hypermethylation (at 10 not 7 days of differentiation) in aged cells (see Figure 5c).
647 Overall, HOXB1, HOXC-AS3 and HOXA3 demonstrated an inverse relationship with CpG methylation and gene
648 expression in aged versus young cells.



649

650 **Figure 6.** Gene expression of the HOX family of genes in aged compared to young muscle stem cells at 7 days of differentiation.

651 *Effect of physical activity on methylation status of HOX family genes*

652 Next, given that aging generally hypermethylated the genome, we tested the hypothesis that increasing
653 physical activity may oppositely regulate DNA methylation and be associated with increasing
654 hypomethylation in these HOX genes. We thus performed a multiple regression analysis using methylation
655 data and the level of physical activity of 30 endurance-trained men. As in the above analysis, we also found
656 that CpG-sites associated with physical activity ($P < 0.05$) were significantly enriched with HOX genes (137 of
657 1219 CpG-sites, Fisher's exact test $OR = 1.7$, $P = 2.3 \times 10^{-8}$, Suppl. File **10a**). Where we determined that highly
658 active men had hypomethylated HOXB1 (cg10558129, $P = 5.2 \times 10^{-4}$), HOXA3 (cg16406967, $P = 0.03$), HOXD12
659 (cg17512364, $P = 0.008$) and HOXC4 gene (cg13826247, $P = 0.014$) compared to less active men (adjusted for
660 age and muscle fiber composition) on the same sites identified above in the aging data. Furthermore, we
661 identified hypomethylation of HOXA3 on several additional sites (cg21134232, $P = 0.0014$, cg25768734,
662 $P = 0.0002$; cg27539480, $P = 0.039$; cg00431187, $P = 0.026$; cg03483713, $P = 0.045$; cg15982700, $P = 0.026$;
663 cg23806243, $P = 0.013$). Full methylome analysis of the physical activity dataset can be found in Suppl. File
664 **10b**, with details of all HOX sites in Suppl. File **10a**). Given that we identified the opposite trend in aged muscle
665 and cells, particularly *HOXB1* and *HOXA3* that were hypermethylated in aged tissue and stem cells, and with
666 reduced gene expression in aged cells. These findings suggest that increasing levels of physical activity are
667 associated with increasing reductions in methylation (hypomethylation) in these HOX genes compared to
668 age-related changes that are associated with increasing methylation (hypermethylation).

669

670 **Discussion**

671

672 In the present study we first aimed to investigate the methylome in aged skeletal muscle tissue and
673 differentiating primary muscle stem cells compared with young adults, in order to identify important
674 epigenetically regulated genes in both aging skeletal muscle tissue and muscle derived stem cells. As with
675 previous studies^{18, 27}, and by using more recent, higher coverage array technology, we identified that aged
676 skeletal muscle tissue demonstrated a considerably hypermethylated profile compared with young adult
677 tissue. We also demonstrated that these hypermethylated profiles in aged tissue were enriched in gene
678 ontology pathways including, 'regulation of muscle system process' and KEGG pathways 'pathways in cancer',
679 a pathway that incorporates previously well described molecular pathways in the regulation of skeletal
680 muscle such as; focal adhesion, MAPK signaling, PI3K-Akt-mTOR signaling, p53 signaling, Jak-STAT signaling,
681 TGF-beta and Notch signaling, as well as the other significantly enriched pathways of 'rap1 signaling', 'axon
682 guidance', and 'hippo signaling'. This was also the first study to profile DNA methylation over the entire time-
683 course of skeletal muscle differentiation (0, 72 h, 7 and 10 d) using the highest coverage 850K methylation
684 assays. In primary cell cultures, isolated from aged and young adults matched for the proportion of myogenic
685 cells, we identified that aged muscle stem cells also demonstrated hypermethylated profiles versus young

686 adult cells. This hypermethylation was enriched in: 'axon guidance', 'adherens junction' and 'calcium
687 signaling' pathways. Furthermore, we identified that the process of cellular differentiation itself did not
688 significantly affect DNA methylation in young cells, however aged cells demonstrated varied methylation
689 profiles particularly at 7 d of differentiation in GO terms: 'regulation of localisation', 'regulation of cell
690 communication', and 'regulation of signaling'. Also, in the majority of different CpG sites that were altered
691 during the process of differentiation, aged cells demonstrated significantly hypermethylated profiles during
692 differentiation when compared with young adult cells. Again, specifically at 7 d of differentiation including
693 CpG's located within: 'focal adhesion', 'adherens junction' and 'regulation of actin cytoskeleton' pathways,
694 as well as the well-known muscle differentiation pathway, 'PI3K-AKT signalling'. This corresponded with
695 reductions in myoD and myogenin, and delayed increases in myogenin gene expression in aged compared
696 with young adult cells.

697
698 We were also able to identify that a small number of CpG sites hypermethylated in aged tissue were also
699 hypermethylated in aged cells, with CpG's located on genes: KIF15, DYRK2, FHL2, MRPS33, ABCA17P. This
700 suggested, that perhaps these CpG's retained their methylation status *in-vitro* after being isolated from the
701 *in-vivo* niche. However, it is worth noting that this was a very small number of CpG's compared with the
702 thousands of CpG sites significantly differentially methylated in the aged tissue versus young adult tissue,
703 and those also observed to be significantly different in the aged versus young muscle cells. This was
704 suggestive that the majority of the hypermethylated CpG's observed at the aged tissue level were generally
705 not retained on the same CpG sites in the isolated aged muscle stem cells *in-vitro*. Also, PCA plots of muscle
706 tissue versus isolated muscle cells demonstrated vastly different profiles, suggesting that isolated cells, even
707 late differentiated muscle cells, are perhaps really quite different epigenetic representations of contrasting
708 cellular entities versus muscle tissue. This also perhaps indicates that hypermethylation of DNA within
709 myonuclei (the predominant source of DNA in the tissue samples) maybe therefore unique to that observed
710 in the isolated aged muscle progenitor cells in combination with other muscle derived cell populations.
711 Indeed, retention of methylation during aging has been previously observed in artificially aged muscle cells
712 ¹⁹. In skeletal muscle tissue, retention of DNA methylation has been observed after skeletal muscle growth,
713 even after a subsequent period of muscle loss, suggesting an epigenetic memory at the DNA methylation
714 level ^{21, 22, 49}. However, the relative contribution of methylation from myonuclei or satellite cells (or other
715 resident cell types in muscle tissue) to this epigenetic memory effect, and how long these retained profiles
716 can last (e.g. past 22 weeks in the Seaborne *et al.*, 2018 study) has not been determined. However,
717 interestingly based on the present studies data, we could hypothesise that myonuclear hypermethylation in
718 the tissue with age is quite different to the hypermethylation observed in muscle progenitor cells as they
719 differentiate. Perhaps, suggesting that environmental stimuli and aging could affect methylation profiles in
720 the myonuclei differently than those in satellite cells. A hypothesis that requires further investigation,
721 perhaps using single-cell DNA/RNA analysis of the different cell populations resident in cells derived from

722 skeletal muscle tissue biopsies compared with cultured cells. Finally, it is important to mention that the
723 human derived muscle cells were comprised of both muscle and non-muscle cells in an attempt to capture
724 the changes across the skeletal muscle 'milieu' of cell types. Therefore, methylation profiles reflect both the
725 differentiation of muscle cells but also expansion predominantly fibrogenic and a minority of other adherent
726 muscle derived cells. As suggested above, with respect to specific methylation changes in myonuclei versus
727 satellite cells, it will be important in future studies to undertake single-cell DNA/RNA analysis to identify the
728 specific contribution of different cell types to the methylation profiles observed in aged cells. Indeed, exciting
729 recent work suggests different methylation profiles from myonuclear versus interstitial cells in response to a
730 hypertrophic stimulus in skeletal muscle ⁶².

731

732 Importantly, in both tissue and stem cell analysis, we also identified that the homeobox (HOX) family of genes
733 were significantly enriched in differentially methylated region analysis, showing several (e.g. 6-8) CpGs to be
734 methylated within chromosomal regions on these genes in aged compared with young adults. In particular,
735 we identified: HOXC10 (just upstream of HOXC6) and HOXB1 as having several CpGs differentially
736 methylated. Therefore, closer analysis of all HOX gene associated CpG changes across both tissue and cell
737 differentiation data identified that CpG's located within: HOXD10, HOXD9, HOXD8, HOXA3, HOXC9, HOXB1,
738 HOXB3, HOXC-AS2 and HOXC10 were all significantly differentially methylated across these analyses. In aged
739 tissue the majority of these HOX genes were hypermethylated. In the cell analysis, these HOX genes displayed
740 the most varied methylation at 7 days of differentiation in aged versus young cells. Furthermore, distinct
741 HOX genes were hypermethylated (HOXD8, HOXC9, HOXB1) and hypomethylated (HOXC10, HOXC-AS2) at 7
742 days in aged cells versus young adult cells. Gene expression analysis also demonstrated an inverse
743 relationship with DNA methylation. Where hypermethylation of HOXB1 and HOXA3 was associated with
744 reduced gene expression, and hypomethylation of HOXC-AS3 associated with increased gene expression in
745 aged versus young cells.

746

747 HOX genes are evolutionary conserved members of the homeobox superfamily, with 39 HOX genes found in
748 the mammalian genome. They are 'homeotic' genes coding for transcription factors, with a fundamental role
749 in the determination of cellular identity. They were first shown to be important in embryogenesis in
750 *drosophila melanogaster* (fruit fly) ⁶³. HOX genes have also been reported to alter with age in non-muscle
751 tissues ^{64, 65}. In muscle they have been described to morphologically identify the hindlimb tissues during
752 development ^{66, 67, 68, 69}, but have also been demonstrated to be activated in satellite cells ^{70, 71, 72}, and as
753 markers of hindlimb derived myoblasts ⁷⁰. In particular HOXC10, demonstrated 8 CpG's, just upstream of
754 HOXC6 and miR-196; Chr12:54383692-54385621, 1933 bp that all demonstrated a hypomethylated signature
755 in aged versus young muscle stem cells. Where miR-196 has previously been demonstrated to regulate HOX
756 gene expression in adipose tissue ⁷³. There were also 4 CpG sites hypomethylated, particularly at 7 days of
757 differentiation in aged versus young cells. Indeed, HOXC10 has been identified to determine hindlimb identity

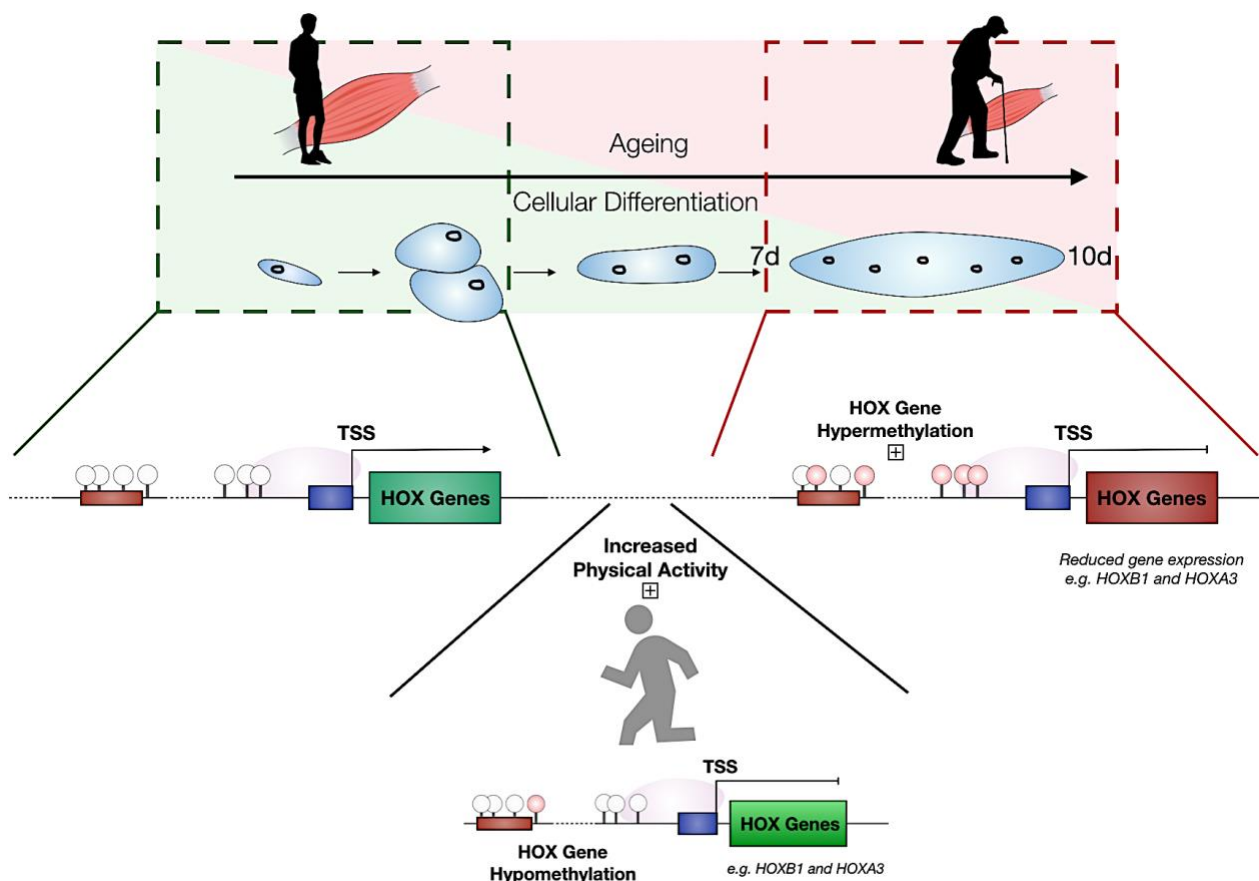
758 ^{66, 68}. Together with HOXC10 hypomethylation, we also demonstrated average (yet not significant) increases
759 in HOXC10 gene expression at 7 days in aged cells versus young cells. Counterintuitively to our data,
760 previously HOXC10 upregulation has been associated with satellite cell activation in skeletal muscle in
761 response to Roux-en-Y gastric bypass (RYGB) surgery ⁷⁴, as well as being a marker for hindlimb specific
762 satellite cells. Interestingly, there was lower expression of HOXC10 observed in exercised rats ⁷⁵, which is
763 perhaps more intuitive with the data provided here, where aged cells demonstrated an increase. However,
764 HOXC10 requires more experimentation to define its mechanistic role in aging skeletal muscle, with HOXC10
765 and physical exercise being discussed below. Interestingly, the hypomethylation of the HOXC10
766 (Chr12:54383692-54385621, 1933 bp) occurred in 8 CpG's on the same chromosome just upstream of the
767 HOXC10 gene (Chr12:54376020-54377868, 1849 bp), within the lncRNA HOXC-AS3, where there were
768 another 6 CpG's that were hypomethylated in aged cells versus young cells (See Suppl. Figure **10** for
769 visualisation of HOXC10 and HOXC-AS3 and their methylation and genomic location). HOXC-AS3 is a long
770 coding RNA (lcrRNA) with currently no known data in skeletal muscle, with some literature in cancer and
771 mesenchymal stem cell (MSC) fields ⁷⁶. Indeed, MSC's administered with silencing HOXC-AS3 prevented bone
772 loss by enhancing HOXC10 expression ⁷⁷, and HOXC-AS3 upregulation has also been linked with aggressive
773 cancer ⁷⁸. Interestingly, we were able to identify that together with associated hypomethylation, in a region
774 close to the lcrRNA HOXC-AS3, there was significantly increased gene expression of HOXC-AS3 (and an
775 average, yet not significant increase in HOXC10 gene expression) in aged muscle cells at 7 days of
776 differentiation. Given the data above in bone and cancer, HOXC-AS3 upregulation appears to be pro-growth
777 and linked with expression of HOXC10, therefore their increase in the current study maybe hypothesised to
778 be a co-operative and compensatory drive to maintain aged muscle. However, this hypothesis is speculative,
779 and more work needs to be conducted as to the role of HOXC10 and HOXC-AS3 and their potential
780 cooperative mechanisms of action in aged skeletal muscle.

781
782 We also identified that HOXB1 was hypermethylated with increased gene expression in aged cells at 7 days.
783 HOXB1 has been demonstrated to be hypermethylated in inflamed muscle of children with Juvenile
784 Dermatomyositis (JDM) ⁷⁹. This is interesting given aged skeletal muscle is known to be chronically inflamed
785 ^{80, 81}, where we also demonstrate this hypermethylated profile in aged cells. HOXA3 was hypermethylated
786 with reduced gene expression in aged cells. However, there is currently little to no work on this gene in
787 skeletal muscle ⁶⁹ and therefore this requires future investigation. It is however worth noting that gene
788 expression, in the aged tissue in particular, was not expected given the methylation data. Where aged tissue
789 demonstrated an increase in gene expression of HOX genes with the majority demonstrating
790 hypermethylation. This may be due one of the elderly patients' donors demonstrated much greater
791 expression versus all the other donors for some of the HOX genes. Therefore, in order to confirm this HOX
792 gene expression would require confirmation in a larger population of aged patients. Other limitations to the
793 study include a mixed cohort of male and female aged individuals compared to the young adult group being

794 all male. PCA analysis of male and female aged samples did not show differences between methylation
795 profiles and we also removed sex (X and Y) chromosome probes from the analysis. Furthermore, the muscle
796 tissue and cells were isolated from two sites, the gluteus medius and vastus lateralis in the aged samples
797 compared with only the vastus lateralis in the young adult samples. This is important to note as the gluteus
798 medius and vastus lateralis have different fibre type proportions. Therefore, the data should be viewed with
799 that caveat in mind. Despite this, the changes in methylation of the sites observed were identified across
800 samples from both biopsy sites, suggesting that these changes occurred in aged individuals across muscle
801 types.

802

803 Finally, with aging evoking a hypermethylated signature in tissue and aged muscle derived stem cells, it was
804 also interesting to speculate that physical exercise, that has been shown to hypomethylate the genome ^{20, 21,}
805 ²², could therefore be ‘anti-ageing’ at the epigenetic level. Indeed, this hypothesis was supported indirectly
806 in the present study and by previous literature, where the aged tissue analysis in the present study identified
807 the top significantly enriched KEGG pathway as, ‘pathways in cancer’. A pathway that incorporates well
808 known pathways important in skeletal muscle, including: Focal adhesion, MAPK, PI3K-Akt, mTOR, p53
809 signaling, Jak-STAT, TGF-beta and Notch signaling. Where, this pathway was also the top enriched
810 hypomethylated pathway after acute and chronic resistance exercise ²². While, perhaps the significance of
811 these larger pathways such as ‘pathways in cancer’ can be inflated in methylation analysis ⁸², and therefore
812 should be viewed with some caution. This data perhaps suggests that exercise (resistance exercise) could
813 perhaps reverse the hypermethylated profiles in these pathways in aged muscle. Therefore, in the present
814 study, given that we identified the HOX family of genes to be extensively differentially methylated in aged
815 tissue and stem cells, we went on to determine that increasing physical activity levels (endurance exercise)
816 in healthy young adults was associated with larger reductions in HOXB1 and HOXA3 methylation
817 (hypomethylation). This was opposite to the changes we observed with age in both muscle tissue and stem
818 cells, that demonstrated increased hypermethylation with age. This also provided evidence to suggest that
819 increased physical activity could perhaps reverse the age-related epigenetic changes in the HOX genes.
820 Importantly, HOXA3 has been shown to be hypomethylated on multiple sites after resistance exercise
821 training, with retention of hypomethylation for site (cg12434681) during detraining into retraining ²¹.
822 Suggesting, that this HOX gene is also hypomethylated with exercise training and possesses an epigenetic
823 memory from earlier exercise training as previously described by our group ⁶⁰. Unpublished work by our
824 group also suggests that acute sprint exercise in human muscle can hypomethylated the same HOXA3 CpG
825 site (cg00431187) that was oppositely hypermethylated in aging but demonstrated hypomethylation in
826 individuals that have higher physical activity level. However, more research into the effect of exercise in an
827 aged population and the changes in HOX methylation status will be required in the future to confirm these
828 findings. Our overarching main results from this study are summarised schematically in Figure 7.



829

830

831

832 **Figure 7.** Schematic of the overarching main results. Hypermethylation of the genome and of the HOX genes in aging skeletal muscle
 833 tissue (RED box) compared with young adult tissue (GREEN BOX). Dysregulation of HOX genes in aged cells particularly at 7 days of
 834 differentiation in muscle derived cells. Inverse methylation (hypermethylation- red circles) with gene expression (reduced- red
 835 rectangle) in aging cells particularly for *HOXB1* and *HOXA3*. Increased physical activity levels are associated with the hypomethylation
 836 (fewer red circles more white circles) of the same two genes, *HOXB1* and *HOXA3*.

837 **Conclusion**

838 Overall, for the first time, we demonstrate that altered methylation of a large number of the HOX genes are
 839 epigenetically differentially regulated in aged human skeletal muscle tissue and during impaired
 840 differentiation in aged muscle stem cells. In particular *HOXB1*, *HOXA3* and *HOXC-AS3* (and to a certain extent,
 841 *HOXC10*) also demonstrated significantly inversed changes in gene expression in aged cells. Finally, that
 842 increased physical activity may help prevent the age-related epigenetic changes observed in these HOX genes

843

844 **Acknowledgments and funding**

845 These data were supported by a North Staffordshire Medical Institute (NMSI) grant awarded to Adam P.
 846 Sharples (PI), Daniel Turner, Mark Kitchen and Ian Dos-Remedios (Co-I's). This work was also supported by
 847 the UK's Engineering and Physical Sciences Research Council (EPSRC) and the UK Medical Research Council's
 848 (MRC) centre for doctoral training, via a studentship awarded to the joint first author Piotr Gorski in the
 849 group of Adam P. Sharples (PI). Funds from Keele University and Liverpool John Moores University, UK and

850 The Norwegian School of Sport Sciences, Oslo, Norway also supported the PhD work by Daniel Turner & Piotr
851 Gorski in the group of Adam P. Sharples. Philipp Baumert received a fully-funded Liverpool John Moores PhD
852 scholarship. Mohd Firdaus Maasar received a PhD studentship via the Malaysian government agency: Majlis
853 Amanah Rakyat (MARA) via Barry Drust, Adam P. Sharples and Dr. Andrew Hulten. The physical activity and
854 DNA methylation study was supported in part by grant from the Russian Science Foundation (Grant No. 17-
855 15-01436: "Comprehensive analysis of the contribution of genetic, epigenetic and environmental factors in
856 the individual variability of the composition of human muscle fibers"; DNA sample collection, genotyping,
857 epigenetic analysis and muscle fibre typing of Russian subjects).

858

859 **Declaration**

860 All authors declare no conflicts of interest.

861

862 **References**

863

- 864 1. Sharples AP, Hughes DC, Deane CS, Saini A, Selman C, Stewart CE. Longevity and skeletal muscle
865 mass: the role of IGF signalling, the sirtuins, dietary restriction and protein intake. *Aging cell* **14**, 511-
866 523 (2015).
867
- 868 2. Morley JE, Anker SD, von Haehling S. Prevalence, incidence, and clinical impact of sarcopenia: facts,
869 numbers, and epidemiology-update 2014. *Journal of cachexia, sarcopenia and muscle* **5**, 253-259
870 (2014).
871
- 872 3. Shafiee G, Keshtkar A, Soltani A, Ahadi Z, Larijani B, Heshmat R. Prevalence of sarcopenia in the world:
873 a systematic review and meta- analysis of general population studies. *J Diabetes Metab Disord* **16**,
874 21 (2017).
875
- 876 4. Hughes VA, *et al.* Longitudinal muscle strength changes in older adults: influence of muscle mass,
877 physical activity, and health. *Journals of Gerontology Series A-Biological Sciences & Medical Sciences*
878 **56**, B209-217 (2001).
879
- 880 5. Cruz-Jentoft AJ, *et al.* Sarcopenia: European consensus on definition and diagnosis: Report of the
881 European Working Group on Sarcopenia in Older People. *Age Ageing* **39**, 412-423 (2010).
882
- 883 6. Hairi NN, *et al.* Loss of muscle strength, mass (sarcopenia), and quality (specific force) and its
884 relationship with functional limitation and physical disability: the Concord Health and Ageing in Men
885 Project. *Journal of the American Geriatrics Society* **58**, 2055-2062 (2010).
886
- 887 7. Cederholm T, Cruz-Jentoft AJ, Maggi S. Sarcopenia and fragility fractures. *European journal of*
888 *physical and rehabilitation medicine* **49**, 111-117 (2013).
889
- 890 8. Cooper C, *et al.* Tools in the assessment of sarcopenia. *Calcified tissue international* **93**, 201-210
891 (2013).
892
- 893 9. Porter MM, Vandervoort AA, Lexell J. Aging of human muscle: structure, function and adaptability.
894 *Scandinavian journal of medicine & science in sports* **5**, 129-142 (1995).
895

- 896 10. Cruz-Jentoft AJ, Landi F, Topinkova E, Michel JP. Understanding sarcopenia as a geriatric syndrome.
897 *Current opinion in clinical nutrition and metabolic care* **13**, 1-7 (2010).
898
- 899 11. Beaudart C, Zaaria M, Pasleau F, Reginster J-Y, Bruyère O. Health Outcomes of Sarcopenia: A
900 Systematic Review and Meta-Analysis. *PLoS ONE* **12**, e0169548 (2017).
901
- 902 12. Fuggle N, Shaw S, Dennison E, Cooper C. Sarcopenia. *Best Pract Res Clin Rheumatol* **31**, 218-242
903 (2017).
904
- 905 13. Sharples AP, Stewart CE, Seaborne RA. Does skeletal muscle have an 'epi'-memory? The role of
906 epigenetics in nutritional programming, metabolic disease, aging and exercise. *Aging cell* **15**, 603-
907 616 (2016).
908
- 909 14. Sharples AP, Seaborne RA, Stewart CE. Epigenetics of Skeletal Muscle Aging. In: *Epigenetics of Aging*
910 *and Longevity* (ed Vaiserman AM). Academic Press (2018).
911
- 912 15. Day K, *et al.* Differential DNA methylation with age displays both common and dynamic features
913 across human tissues that are influenced by CpG landscape. *Genome biology* **14**, R102 (2013).
914
- 915 16. Voisin S, *et al.* An epigenetic clock for human skeletal muscle. *Journal of cachexia, sarcopenia and*
916 *muscle*, Epub DOI 10.1002/jcsm.12556 (2020).
917
- 918 17. Horvath S. DNA methylation age of human tissues and cell types. *Genome biology* **14**, 3156 (2013).
919
- 920 18. Zykovich A, *et al.* Genome-wide DNA methylation changes with age in disease-free human skeletal
921 muscle. *Aging cell* **13**, 360-366 (2014).
922
- 923 19. Sharples AP, Polydorou I, Hughes DC, Owens DJ, Hughes TM, Stewart CE. Skeletal muscle cells possess
924 a 'memory' of acute early life TNF- α exposure: role of epigenetic adaptation. *Biogerontology* **17**,
925 603-617 (2016).
926
- 927 20. Sailani MR, *et al.* Lifelong physical activity is associated with promoter hypomethylation of genes
928 involved in metabolism, myogenesis, contractile properties and oxidative stress resistance in aged
929 human skeletal muscle. *Scientific reports* **9**, 3272 (2019).
930
- 931 21. Seaborne RA, *et al.* Human Skeletal Muscle Possesses an Epigenetic Memory of Hypertrophy.
932 *Scientific Reports (Nature)* **8**, 1898 (2018).
933
- 934 22. Turner DC, Seaborne RA, Sharples AP. Comparative Transcriptome and Methylome Analysis in
935 Human Skeletal Muscle Anabolism, Hypertrophy and Epigenetic Memory. *Scientific reports* **9**, 4251
936 (2019).
937
- 938 23. Tsumagari K, *et al.* Early de novo DNA methylation and prolonged demethylation in the muscle
939 lineage. *Epigenetics : official journal of the DNA Methylation Society* **8**, 317-332 (2013).
940
- 941 24. Brunk BP, Goldhamer DJ, Emerson JCP. Regulated Demethylation of the myoD Distal Enhancer during
942 Skeletal Myogenesis. *Developmental Biology* **177**, 490-503 (1996).
943
- 944 25. Fuso A, *et al.* Early demethylation of non-CpG, CpC-rich, elements in the myogenin 5'-flanking region:
945 a priming effect on the spreading of active demethylation. *Cell Cycle* **9**, 3965-3976 (2010).
946
- 947 26. Wu W, Ren Z, Wang Y, Chao Z, Xu D, Xiong Y. Molecular characterization, expression patterns and
948 polymorphism analysis of porcine Six1 gene. *Molecular Biology Reports* **38**, 2619-2632 (2011).
949

- 950 27. Bigot A, *et al.* Age-Associated Methylation Suppresses SPRY1, Leading to a Failure of Re-quiescence
951 and Loss of the Reserve Stem Cell Pool in Elderly Muscle. *Cell reports* **13**, 1172-1182 (2015).
952
- 953 28. Barberi L, *et al.* Age-dependent alteration in muscle regeneration: the critical role of tissue niche.
954 *Biogerontology* **14**, 273-292 (2013).
955
- 956 29. Hidestrand M, *et al.* Sca-1-expressing nonmyogenic cells contribute to fibrosis in aged skeletal
957 muscle. *J Gerontol A Biol Sci Med Sci* **63**, 566-579 (2008).
958
- 959 30. Pietrangelo T, Puglielli C, Mancinelli R, Beccafico S, Fano G, Fulle S. Molecular basis of the myogenic
960 profile of aged human skeletal muscle satellite cells during differentiation. *Exp Gerontol* **44**, 523-531
961 (2009).
962
- 963 31. Beccafico S, *et al.* Human muscle satellite cells show age-related differential expression of S100B
964 protein and RAGE. *Age (Dordr)* **33**, 523-541 (2010).
965
- 966 32. Sharples AP, Al-Shanti N, Stewart CE. C2 and C2C12 murine skeletal myoblast models of atrophic and
967 hypertrophic potential: relevance to disease and ageing? *J Cell Physiol* **225**, 240-250 (2010).
968
- 969 33. Sharples AP, Al-Shanti N, Lewis MP, Stewart CE. Reduction of myoblast differentiation following
970 multiple population doublings in mouse C2 C12 cells: a model to investigate ageing? *Journal of*
971 *cellular biochemistry* **112**, 3773-3785 (2011).
972
- 973 34. Sharples AP, Player DJ, Martin NR, Mudera V, Stewart CE, Lewis MP. Modelling in vivo skeletal muscle
974 ageing in vitro using three-dimensional bioengineered constructs. *Aging Cell* **11**, 986-995 (2012).
975
- 976 35. Merritt EK, *et al.* Heightened muscle inflammation susceptibility may impair regenerative capacity in
977 aging humans. *J Appl Physiol* **115**, 937-948 (2013).
978
- 979 36. Zwetsloot KA, Childs TE, Gilpin LT, Booth FW. Non-passaged muscle precursor cells from 32-month
980 old rat skeletal muscle have delayed proliferation and differentiation. *Cell Prolif* **46**, 45-57 (2013).
981
- 982 37. Bigot A, *et al.* Replicative aging down-regulates the myogenic regulatory factors in human myoblasts.
983 *Biol Cell* **100**, 189-199 (2008).
984
- 985 38. Carlson ME, Conboy IM. Loss of stem cell regenerative capacity within aged niches. *Aging cell* **6**, 371-
986 382 (2007).
987
- 988 39. Lancioni H, Lucentini L, Palomba A, Fulle S, Micheli MR, Panara F. Muscle actin isoforms are
989 differentially expressed in human satellite cells isolated from donors of different ages. *Cell biology*
990 *international* **31**, 180-185 (2007).
991
- 992 40. Lees SJ, Rathbone CR, Booth FW. Age-associated decrease in muscle precursor cell differentiation.
993 *Am J Physiol Cell Physiol* **290**, C609-615 (2006).
994
- 995 41. Lorenzon P, *et al.* Ageing affects the differentiation potential of human myoblasts. *Exp Gerontol* **39**,
996 1545-1554 (2004).
997
- 998 42. Charge SB, Brack AS, Hughes SM. Aging-related satellite cell differentiation defect occurs
999 prematurely after Ski-induced muscle hypertrophy. *Am J Physiol Cell Physiol* **283**, C1228-1241 (2002).
1000
- 1001 43. Allen RE, McAllister PK, Masak KC, Anderson GR. Influence of age on accumulation of alpha-actin in
1002 satellite-cell-derived myotubes in vitro. *Mech Ageing Dev* **18**, 89-95 (1982).
1003

- 1004 44. Kandalla PK, Goldspink G, Butler-Browne G, Mouly V. Mechano Growth Factor E peptide (MGF-E),
1005 derived from an isoform of IGF-1, activates human muscle progenitor cells and induces an increase
1006 in their fusion potential at different ages. *Mech Ageing Dev* **132**, 154-162 (2011).
1007
- 1008 45. Corbu A, *et al.* Satellite cell characterization from aging human muscle. *Neurological research* **32**, 63-
1009 72 (2010).
1010
- 1011 46. Shefer G, Van de Mark DP, Richardson JB, Yablonka-Reuveni Z. Satellite-cell pool size does matter:
1012 defining the myogenic potency of aging skeletal muscle. *Developmental Biology* **294**, 55-66 (2006).
1013
- 1014 47. Alsharidah M, Lazarus NR, George TE, Agle CC, Velloso CP, Harridge SD. Primary human muscle
1015 precursor cells obtained from young and old donors produce similar proliferative, differentiation and
1016 senescent profiles in culture. *Aging cell* **12**, 333-344 (2013).
1017
- 1018 48. Seaborne RA, *et al.* UBR5 is a novel E3 ubiquitin ligase involved in skeletal muscle hypertrophy and
1019 recovery from atrophy. *J Physiol* **597**, 3727-3749 (2019).
1020
- 1021 49. Seaborne RA, *et al.* Methylome of human skeletal muscle after acute & chronic resistance exercise
1022 training, detraining & retraining. *Scientific Data (Nature)* **5**, 180213 (2018).
1023
- 1024 50. Turner DC, *et al.* Exercising Bioengineered Skeletal Muscle In Vitro: Biopsy to Bioreactor. In: *Methods*
1025 *in Molecular Biology*) (2019).
1026
- 1027 51. Turner DC, *et al.* UBR5 knockdown in human myotubes in-vitro and mouse skeletal muscle tissue in-
1028 vivo determines its pertinent role in anabolism and hypertrophy. *bioRxiv*, DOI: DOI:
1029 10.1101/2020.06.05.116145 (2020).
1030
- 1031 52. Altıntaş A, Laker RC, Garde C, Barrès R, Zierath JR. Transcriptomic and epigenomics atlas of myotubes
1032 reveals insight into the circadian control of metabolism and development. *Epigenomics* **12**, 701-713
1033 (2020).
1034
- 1035 53. Maksimovic J, Phipson B, Oshlack A. A cross-package Bioconductor workflow for analysing
1036 methylation array data [version 1; referees: 3 approved, 1 approved with reservations].
1037 *F1000Research* **5**, (2016).
1038
- 1039 54. Pidsley R, *et al.* Critical evaluation of the Illumina MethylationEPIC BeadChip microarray for whole-
1040 genome DNA methylation profiling. *Genome biology* **17**, 208 (2016).
1041
- 1042 55. Maksimovic J, Gordon L, Oshlack A. SWAN: Subset-quantile within array normalization for illumina
1043 infinium HumanMethylation450 BeadChips. *Genome Biol* **13**, R44 (2012).
1044
- 1045 56. Du P, *et al.* Comparison of Beta-value and M-value methods for quantifying methylation levels by
1046 microarray analysis. *BMC Bioinformatics* **11**, 587 (2010).
1047
- 1048 57. Kanehisa M, Goto S. KEGG: kyoto encyclopedia of genes and genomes. *Nucleic Acids Res* **28**, 27-30
1049 (2000).
1050
- 1051 58. Kanehisa M, Furumichi M, Tanabe M, Sato Y, Morishima K. KEGG: new perspectives on genomes,
1052 pathways, diseases and drugs. *Nucleic Acids Res* **45**, D353-d361 (2017).
1053
- 1054 59. Kanehisa M, Sato Y, Kawashima M, Furumichi M, Tanabe M. KEGG as a reference resource for gene
1055 and protein annotation. *Nucleic Acids Res* **44**, D457-462 (2016).
1056

- 1057 60. Schmittgen TD, Livak KJ. Analyzing real-time PCR data by the comparative C(T) method. *Nature*
1058 *protocols* **3**, 1101-1108 (2008).
1059
- 1060 61. McCartney DL, Walker RM, Morris SW, McIntosh AM, Porteous DJ, Evans KL. Identification of
1061 polymorphic and off-target probe binding sites on the Illumina Infinium MethylationEPIC BeadChip.
1062 *Genomics Data* **9**, 22-24 (2016).
1063
- 1064 62. Von Walden F, *et al.* The myonuclear DNA methylome in response to an acute hypertrophic stimulus.
1065 *Epigenetics : official journal of the DNA Methylation Society*, 1-12 (2020).
1066
- 1067 63. Shah N, Sukumar S. The Hox genes and their roles in oncogenesis. *Nat Rev Cancer* **10**, 361-371 (2010).
1068
- 1069 64. Morgan R, Begum R, Theti D, Chansa M, Pettengell R, Sohal J. HOXA9 expression increases with age
1070 in human haemopoietic cells. *Leukemia Research* **29**, 1221-1222 (2005).
1071
- 1072 65. Yau C, *et al.* Aging impacts transcriptomes but not genomes of hormone-dependent breast cancers.
1073 *Breast Cancer Res* **9**, R59 (2007).
1074
- 1075 66. DeLaurier A, Schweitzer R, Logan M. Pitx1 determines the morphology of muscle, tendon, and bones
1076 of the hindlimb. *Dev Biol* **299**, 22-34 (2006).
1077
- 1078 67. Carpenter EM, Goddard JM, Davis AP, Nguyen TP, Capecchi MR. Targeted disruption of Hoxd-10
1079 affects mouse hindlimb development. *Development* **124**, 4505-4514 (1997).
1080
- 1081 68. Logan M, Tabin CJ. Role of Pitx1 upstream of Tbx4 in specification of hindlimb identity. *Science* **283**,
1082 1736-1739 (1999).
1083
- 1084 69. Manley NR, Capecchi MR. Hox group 3 paralogous genes act synergistically in the formation of
1085 somitic and neural crest-derived structures. *Dev Biol* **192**, 274-288 (1997).
1086
- 1087 70. Choi HY, Jeon H, Yang JW, Ahn JH, Jung JH. Thyroid-Stimulating Hormone Receptor Expression on
1088 Primary Cultured Human Extraocular Muscle Myoblasts. *Curr Eye Res* **43**, 1484-1488 (2018).
1089
- 1090 71. Seale P, Ishibashi J, Holterman C, Rudnicki MA. Muscle satellite cell-specific genes identified by
1091 genetic profiling of MyoD-deficient myogenic cell. *Dev Biol* **275**, 287-300 (2004).
1092
- 1093 72. Schwörer S, *et al.* Epigenetic stress responses induce muscle stem-cell ageing by Hoxa9
1094 developmental signals. *Nature* **540**, 428-432 (2016).
1095
- 1096 73. Divoux A, *et al.* MicroRNA-196 Regulates HOX Gene Expression in Human Gluteal Adipose Tissue.
1097 *Obesity (Silver Spring)* **25**, 1375-1383 (2017).
1098
- 1099 74. Tamboli RA, *et al.* Reduction in inflammatory gene expression in skeletal muscle from Roux-en-Y
1100 gastric bypass patients randomized to omentectomy. *PLoS ONE* **6**, e28577 (2011).
1101
- 1102 75. Kato H, Shibahara T, Rahman N, Takakura H, Ohira Y, Izawa T. Effect of a 9-week exercise training
1103 regimen on expression of developmental genes related to growth-dependent fat expansion in
1104 juvenile rats. *Physiological reports* **6**, e13880 (2018).
1105
- 1106 76. Zhang E, *et al.* A novel long noncoding RNA HOXC-AS3 mediates tumorigenesis of gastric cancer by
1107 binding to YBX1. *Genome biology* **19**, 154 (2018).
1108
- 1109 77. Li B, *et al.* HOXC10 Regulates Osteogenesis of Mesenchymal Stromal Cells Through Interaction with
1110 Its Natural Antisense Transcript lncHOXC-AS3. *Stem cells (Dayton, Ohio)* **37**, 247-256 (2019).

- 1111
1112 78. Wang X, *et al.* HOXB13 promotes proliferation, migration, and invasion of glioblastoma through
1113 transcriptional upregulation of lncRNA HOXC-AS3. *Journal of cellular biochemistry* **120**, 15527-15537
1114 (2019).
1115
- 1116 79. Wang M, Xie H, Shrestha S, Sredni S, Morgan GA, Pachman LM. Methylation alterations of WT1 and
1117 homeobox genes in inflamed muscle biopsy samples from patients with untreated juvenile
1118 dermatomyositis suggest self-renewal capacity. *Arthritis and rheumatism* **64**, 3478-3485 (2012).
1119
- 1120 80. Greiwe JS, Cheng B, Rubin DC, Yarasheski KE, Semenkovich CF. Resistance exercise decreases skeletal
1121 muscle tumor necrosis factor alpha in frail elderly humans. *FASEB journal : official publication of the*
1122 *Federation of American Societies for Experimental Biology* **15**, 475-482 (2001).
1123
- 1124 81. Leger B, Derave W, De Bock K, Hespel P, Russell AP. Human sarcopenia reveals an increase in SOCS-
1125 3 and myostatin and a reduced efficiency of Akt phosphorylation. *Rejuvenation research* **11**, 163-
1126 175B (2008).
1127
- 1128 82. Reimand J, *et al.* Pathway enrichment analysis and visualization of omics data using g:Profiler, GSEA,
1129 Cytoscape and EnrichmentMap. *Nature protocols* **14**, 482-517 (2019).
1130
1131